

1 **Water mass-specificity of bacterial communities in the North Atlantic revealed by**
2 **massively parallel sequencing.**

3 Hélène Agogue^{1‡} [⊖], Dominique Lamy^{1,2} [⊖], Phillip R. Neal³, Mitchell L. Sogin³, Gerhard J.
4 Herndl^{1,2*}

5
6 ¹ Dept. of Biological Oceanography, Royal Netherlands Institute for Sea Research (NIOZ), P.O.
7 Box 59, 1790AB Den Burg The Netherlands

8 ² Dept. of Marine Biology, University of Vienna Althanstraße, 14 A-1090 Vienna, Austria

9 ³ Josephine Bay Paul Center for Comparative Molecular Biology and Evolution, Marine
10 Biological Laboratory, 7 MBL Street, Woods Hole, Massachusetts 02543, United States of
11 America

12 [‡]Current address : Institut du Littoral et de l'Environnement, UMR LIENSs 6250, CNRS-
13 Université de la Rochelle, 2 rue Olympes de Gouges, 17000 LA ROCHELLE France

14
15 [⊖] **These authors contributed equally to this work.**

16
17 **Keywords:** bacterial diversity; massively parallel tag sequencing; North Atlantic Ocean; deep
18 water masses, bacterial biogeography

19
20 * To whom correspondence should be addressed:

21 Gerhard J. Herndl
22 Dept. of Marine Biology
23 University of Vienna
24 Althanstraße, 14

25 ,A-1090, Vienna, Austria

26 E-mail: gerhard.herndl@univie.ac.at

27 Fax number: +43(0)1 4277 9571

28

29 **Running title:** Bacterial assemblages in North Atlantic Ocean

30

31 **Abbreviations:** LDW, lower Deep Water; NEADW, Northeast Atlantic Deep Water; SACW,
32 South Atlantic Central Water; LSW, Labrador Sea Water; NIW, Northern Intermediate Water;
33 tCW, transitional Central Water; AAIW, Antarctic Intermediate Water; DOC, dissolved organic
34 carbon; DON, dissolved organic nitrogen; AOU, apparent oxygen utilization; HNA, high nucleic
35 acid; MDS, non-metric multidimensional scaling; CCA, canonical correspondence analysis.

36

37 **ABSTRACT**

38 Bacterial assemblages from subsurface (100 m depth), meso- (200-1000 m depth) and bathy-
39 pelagic (below 1000 m depth) zones at 10 stations along a North Atlantic Ocean transect from
40 60°N to 5°S were characterized using massively parallel pyrotag sequencing of the V6 region of
41 the 16S rRNA gene (V6 pyrotags). In a dataset of more than 830,000 pyrotags we identified
42 10,780 OTUs of which 52% were singletons. The singletons accounted for less than 2% of the
43 OTU abundance, while the 100 and 1,000 most abundant OTUs represented 80% and 96%,
44 respectively, of all recovered OTUs. Non-metric Multi-Dimensional Scaling and Canonical
45 Correspondence Analysis of all the OTUs excluding the singletons revealed a clear clustering of
46 the bacterial communities according to the water masses. More than 80% of the 1,000 most
47 abundant OTUs corresponded to *Proteobacteria* of which 55% were *Alphaproteobacteria*,
48 mostly composed of the SAR11 cluster. *Gammaproteobacteria* increased with depth and
49 included a relatively large number of OTUs belonging to *Alteromonadales* and
50 *Oceanospirillales*. The bathypelagic zone showed higher taxonomic evenness than the overlying
51 waters, albeit bacterial diversity was remarkably variable. Both abundant and low-abundance
52 OTUs were responsible for the distinct bacterial communities characterizing the major deep-
53 water masses. Taken together, our results reveal that deep-water masses act as bio-oceanographic
54 islands for bacterioplankton leading to water mass-specific bacterial communities in the deep
55 waters of the Atlantic.

56

57 INTRODUCTION

58 Prokaryotes represent an important component of the marine plankton, comprising up to
59 70% and 75% of the total biomass in surface (Fuhrman *et al.* 1989) and deep (Aristegui *et al.*
60 2009) waters, respectively. They serve a fundamental role in mediating a wide range of
61 biogeochemical cycles (Azam *et al.* 1983; Karl 2002). The introduction of molecular tools has
62 substantially increased our knowledge about marine microbial community structure and has
63 shown that the vast majority of environmental microbes represents novel taxa that have yet to be
64 cultivated (Handelsman 2004; Olsen *et al.* 1986). High-throughput sequencing methods and
65 pyrosequencing allow for efficient deep molecular sampling efforts of the microbial populations
66 (Gilbert *et al.* 2009; Huber *et al.* 2007; Huse *et al.* 2008; Sogin *et al.* 2006) and sidestep the need
67 to clone individual DNA molecules (Margulies *et al.* 2005). Furthermore, data from these
68 massively parallel sequencing approaches provide an exhaustive description of the taxonomic
69 affiliation of microbial community. This information forms the basis for estimating both the
70 richness and evenness of the microbial populations present in the environment which are, in turn,
71 essential to refine our knowledge on the biogeography of marine microbes (Galand *et al.* 2009b;
72 Galand *et al.* 2010; Martiny *et al.* 2006; Pommier *et al.* 2005) and to relate microbial diversity
73 and ecosystem properties (Andersson *et al.* 2009).

74 By applying a high-throughput pyrosequencing strategy, Sogin *et al.* (2006) found a
75 remarkably high bacterial diversity in the deep-water masses of the North Atlantic and in diffuse
76 flow hydrothermal vents. The study highlighted the existence of thousands of low-abundance
77 populations, coined the “rare biosphere”, which accounted for most of the observed phylogenetic
78 bacterial diversity (Sogin *et al.* 2006). The rare phylotypes are assumed to be recruited by
79 immigration and to have extremely low loss rates from grazing and viral lysis (Pedros-Alio

80 2006). Conventional molecular techniques fail to detect microbial phylotypes that make up the
81 long tail of taxon rank-distribution curves because dominant populations (comprising > 1% of
82 the total community) mask the detection of the highly diverse, low-abundance organisms. The
83 massively parallel pyrotag sequencing approach, however, allows for deep sequencing that can
84 capture information about these low-abundance populations (Galand *et al.* 2009a; Palacios *et al.*
85 2008; Sogin *et al.* 2006).

86 The spatial variability of microbial diversity across habitats has not been investigated
87 extensively (Galand *et al.* 2010; Pommier *et al.* 2007). The availability of resources, selective
88 loss factors (grazing and viral lysis), and physical parameters such as temperature and salinity
89 can influence microbial population structure. This is in accordance with the deterministic theory
90 “everything is everywhere, but, the environment selects” (Baas Becking 1934) which has been
91 debated extensively recently (de Wit & Bouvier 2006; O'Malley 2008). In contrast, stochastic
92 neutral models of biodiversity and biogeography (Hubbel 2001; Sloan *et al.* 2006) postulate that
93 immigration, dispersal rates, size of the habitat (*i.e.*, taxa-area relationships) (Woodcock *et al.*
94 2007) and ecological invariance among microbial phylotypes shape microbial community
95 structure.

96 Distinct water masses characterize the hydrodynamic conditions of the ocean, most
97 notably the major water masses driving the thermohaline ocean circulation (Tomczak & Godfrey
98 2003). Non-sinking free-living prokaryotes inhabiting oceanic deep waters might be trapped in
99 these distinct water masses leading overall to water mass-specific prokaryotic community
100 composition and activity (Agogu e *et al.* 2008; Galand *et al.* 2009b; Galand *et al.* 2010; Varela *et*
101 *al.* 2008a; Varela *et al.* 2008b). Hence, dispersal and immigration of free-living microbes in the
102 ocean might be more limited than generally assumed. These physical boundary conditions of

103 oceanic water masses might constrain the applicability of some of the fundamental theories and
104 models on the biogeographic distribution of microbes in the ocean.

105 This study aimed at describing the composition of bacterial assemblages in the North
106 Atlantic Ocean throughout the water column by using massively parallel pyrotag sequencing to
107 resolve the spatial distribution of bacterial richness and evenness in different water masses. We
108 hypothesized that the bacterial communities exhibit a biogeography according to the water
109 masses. Hence, we expected that bacterial communities collected several 1000 km apart from
110 each other but originating from the same water mass are more similar than bacterial communities
111 collected less than a few hundred meters apart but from different water masses. We used data
112 from the hypervariable V6 region of the bacterial 16S rRNA gene from 45 samples collected
113 from the main deep water masses along a 8000 km north-to-south transect in North Atlantic
114 Ocean ranging from 60°N to 5°S.

115

116 **MATERIAL AND METHODS**

117 **Study site and sampling.**

118 Sampling was conducted during the cruises TRANSAT-1 (September 2002) and -2 (May 2003)
119 and ARCHIMEDES-2 (November/December 2006) on board R/V *Pelagia* following the North
120 Atlantic Deep Water (NADW) from 60°N to 5°S in the eastern basin of the Atlantic Ocean (Fig.
121 1). Ten stations were occupied, and samples were taken from 6 to 10 sampling depths at each
122 station from 100m to 4500m depth. In total, 45 samples were collected for massively parallel
123 pyrotag sequencing (Table S1).

124 The water masses along the eastern North Atlantic section were identified by their
125 distinct potential temperature and salinity characteristics (Table S2, Fig. S1) (van Aken 2000a,

126 b). At 4000-5000m depth, the Lower Deep Water (LDW) has low salinity (34.9) and temperature
127 (1.9 - 2.6°C) (Table S2, Fig. S1). The NEADW (North East Atlantic Deep Water) is
128 characterized by a temperature between 2.5 and 4.1°C and a higher salinity than LDW (Table S2,
129 Fig. S1). The core of NEADW was identifiable throughout the transect at around 2750m depth.
130 Two types of mesopelagic waters were found in the (sub)equatorial region: the transitional and
131 South Atlantic Central Water (tCW/SACW) exhibiting the same temperature and salinity
132 characteristics, and the Antarctic Intermediate Water (AAIW) characterized by lower salinity and
133 temperature than tCW/SACW (Table S2, Fig. S1). In the northernmost region of the transect, the
134 Northern Intermediate Water (NIW) was found at 500m depth, showing the same temperature
135 but higher salinity than AAIW. Labrador Sea Water (LSW) was clearly identifiable at depths
136 between 1200-2100m throughout the transect (Table S2, Fig. S1). Samples from the distinct
137 water masses were collected with 10-L NOEX (no oxygen exchanges) bottles mounted in a CTD
138 (conductivity, temperature, depth) frame. Samples were collected from: (i) subsurface waters
139 (lower euphotic layer, 100-150m layer), (ii) mesopelagic waters including tCW and SACW (250
140 – 500m layer), AAIW (750 – 900m layer) and NIW (500m), and (iii) bathypelagic waters
141 including LSW (1200 – 2100m layer), NEADW (1750 – 4000m layer) and LDW (4000 – 5000m
142 layer) (Table S1).

143

144 **DNA extraction, pyrosequencing and identification of the bacterial phylotypes**

145 *DNA extraction.* During the TRANSAT cruises, 1 L of seawater from each depth was filtered
146 onto a 0.2 µm polycarbonate filter (Millipore) and the filters were subsequently stored at -80°C
147 until further processing in the lab. During the ARCHIMEDES-2 cruise, 10 L of seawater from
148 each depth was filtered through a 0.22 µm Sterivex filter GP unit (Millipore). Lysis buffer (40

149 mM EDTA, 50 mM Tris-HCl, 0.75 M sucrose) was then added into the Sterivex (1.8 mL) and
150 the filters were subsequently stored at -80°C until analysis. Extraction of total DNA was
151 performed using an UltraClean soil DNA and Mega soil DNA isolation kit (Mobio) for
152 TRANSAT-1 & -2 and ARCHIMEDES-2 samples, respectively.

153 *PCR amplicon library construction and pyrosequencing.* The hypervariable V6 region of the 16S
154 rRNA of bacteria was amplified from TRANSAT samples using primers 967F, 5'-
155 gcctccctcgcgcatcag-CAACGCGAAGAACCTTACC-3' and 1046R, 5'-gccttgccagcccgcctcag-
156 CGACAGCCATGCANACCT-3' and pyrosequenced on a Roche Genome Sequencer 20 under
157 conditions described in Sogin *et al.* (2006). A cocktail of five fused primers at the 5' end of the
158 V6 region (*E. coli* positions 967- 985) and four primers at the 3' end (*E. coli* positions 1046-
159 1028) that capture the full diversity of rRNA sequences represented in molecular databases
160 (Huber *et al.* 2007; Sogin *et al.* 2006) amplified ARCHIMEDES-2 environmental DNA samples
161 for pyrosequencing on a Roche Genome GS FLX system. For both the TRANSAT and
162 ARCHIMEDES-2 we prepared amplicon libraries from at least three independent PCR cocktails
163 to minimize the impact of potential early-round PCR errors. To minimize effects of sequencing
164 errors, we employed a quality trimming procedure to remove low quality pyrotags and to
165 eliminate sequences with multiple undetermined residues or mismatches to the PCR primers at
166 the beginning of a read (Huse *et al.* 2007).

167

168 **Clustering and assignment of the OTUs: identification of bacterial phylotypes.**

169 The clustering of V6 pyrotags into Operational Taxonomic Units (OTUs) was done with
170 the new single-linkage preclustering (SLP) algorithm to smooth sequencing errors and reduce
171 noise, followed by primary pairwise, average linkage clustering (PW-AL) described in Huse *et*

172 *al.* (2010). The advantage of this new method is that it corrects for sequencing errors and
173 minimizes the propagation of OTUs with sequencing effort. This method provides a comparable
174 reduction in spurious OTUs as a previously published algorithm (*e.g.* PyroNoise, Qunice *et al.*
175 2009), but requires less computational expense (Huse *et al.* 2010, see also the Discussion part on
176 pyrosequencing errors). OTUs were created using clustering thresholds of 3% corresponding to
177 97% similarity.

178 We assigned taxonomic identifiers to OTUs by using the rRNA indexing algorithm
179 Global Assignment of Sequence Taxonomy (GAST) (Sogin *et al.* 2006), which compares OTUs
180 to known rRNA genes that have already been placed in a phylogenetic framework of more than
181 1,000,000 nearly full-length rRNA reference sequences (RefSSU) based on the SILVA database
182 (Pruesse *et al.* 2007). GAST methodology is freely available through the VAMPS (Visualisation
183 and Analysis of Microbial Population Structure) website
184 (<http://vamps.mbl.edu/resources/faq.php#gasting>). The V6 reference database (V6RefDB: high-
185 quality, full-length 16S rRNA sequences) is publically available at: <http://vamps.mbl.edu>.

186

187 **Accession numbers and data availability.**

188 The OTU sequences and supporting data have been submitted to the NCBI Short Read
189 Archive (<http://www.ncbi.nlm.nih.gov/Traces/home/>). Run IDs are SRR029056-SRR029102
190 inclusive. One run corresponds to one sample. The sequences obtained from each run are
191 downloadable from the SRA (sequence read archive) web site of NCBI. In addition, the VAMPS
192 site <http://vamps.mbl.edu> provides individual and edited sequences and analytical functions for
193 interrogating the data.

194

195 **Diversity estimation and statistical analysis.**

196 *Diversity indices.* The non-parametric ACE and the Chao1 richness index were calculated with
197 the CatchAll software program (Bunge *et al.* 2010).

198 The Gini index of evenness (Wittebolle *et al.* 2009) was calculated on the relative abundance of
199 all OTUs except the singletons using the ineq function in the ineq package of the software
200 package R for subsurface, meso- and bathypelagic samples. The higher the Gini index is, the
201 more unevenly distributed are the OTUs.

202 *Cluster analysis.* Non-metric multidimensional scaling (MDS) (Kruskal 1964a, b) was used to
203 determine the similarity between samples. This data-reduction method shows the differences (or
204 similarities) between samples by reducing the comparisons between samples from a
205 multidimensional space to fewer dimensions, preferably 2 or 3. Differences between samples
206 were calculated based on the relative abundance of (i) all the OTUs, (ii) all the OTUs except the
207 singletons and (iii) the 1,000 most abundant OTUs. MDS analysis was also applied to (i) all the
208 pyrotags except the singletons, (ii) the abundant pyrotags (frequency > 1% within a sample) and
209 (iii) the rare pyrotags (frequency < 0.01% within a sample). The similarities are presented in a
210 multidimensional space by plotting more similar samples closer together (Kruskal 1964a, b).

211 Analysis of similarity (ANOSIM) was used to verify the significance of the MDS
212 clustering by testing the hypothesis that bacterial communities from the same cluster were more
213 similar to each other than to communities in different clusters. A Bray–Curtis similarity matrix
214 computed from the relative abundance of all OTUs except the singletons was used to generate
215 one-way ANOSIM statistics with 999 permutations.

216 *SIMPER analysis.* Similarity percentage (SIMPER) (Clarke & Warwick 2001) was used to
217 determine which individual sequence contributed most to the dissimilarity between water masses

218 (Dataset S1). The SIMPER analysis was also used to determine the percentage of similarity (i)
219 between each station and the northernmost station of the transect (station 27, Transat-2 cruise)
220 (Fig.1, Table S1) within specific water layers and (ii) between water layers, based on the relative
221 abundance of all OTUs except the singletons. The data of the NEADW from Sogin *et al.* (2006)
222 were included in these analyses to allow full comparison of all the stations occupied from 60°N
223 to 5°S, *i.e.*, a stretch of 8000 km.

224 *Mantel analysis.* The Mantel test was used to analyze the phylogenetic composition of the 1,000
225 most abundant OTUs and the singletons among all the samples. Mantel analysis was also used to
226 determine the relationships between (i) bacterial assemblage structure, (ii) environmental factors
227 and (iii) bacteria-related parameters. The three similarity matrices (Euclidian distance, n = 45)
228 included the following variables: (i) the relative abundance of all OTUs except the singletons,
229 (ii) temperature, salinity, concentration of inorganic nutrients (nitrite, nitrate, ammonia, silicate
230 and phosphate), dissolved organic carbon (DOC) and nitrogen (DON), apparent oxygen
231 utilization (AOU), latitude, longitude and depth and (iii) bacterial-related variables comprising
232 bacterial abundance and production, percentage of high nucleic acid cells (HNA), potential
233 respiration (measured as activity of the electron transport system), alpha- and beta-glucosidase,
234 leucine aminopeptidase and alkaline phosphatase activity and its enzyme kinetics.

235 *CCA analysis.* A canonical correspondence analysis (CCA) was used to investigate the variations
236 in the relative abundance of the 1,000 most abundant OTUs under the constraint of our set of
237 environmental variables. We assumed a unimodal response of OTUs to environmental variations.
238 Generally, nonlinear models are required for analysis of ecological data collected over a large
239 range of habitats (Ter Braak & Verdonschot 1995). When a linear response is assumed, the
240 percentage of explained variation is lower (redundancy analysis not shown). The null hypothesis

241 that the bacterial assemblage is independent of the environmental parameters was tested using
242 constrained ordination with a Monte Carlo permutation test (499 permutations). The parameters
243 were selected to obtain significant canonical axes ($p < 0.05$) and to maximize the percentage of
244 variance explained. The cluster, the SIMPER and the Mantel analyses were performed with
245 PRIMER 6.1.7 (Primer-E, Ltd) and XLSTAT Pro (2006) software. The CCA analysis was
246 performed with the Canoco version 4.5 software (Ter Braak 1989).

247

248 **Variability of the 100 most abundant OTUs per water mass**

249 The deviation (in %) from the mean relative abundance in all the samples was calculated
250 for the 100 most abundant OTUs for the different water masses. This deviation was calculated
251 for each water mass and for each of the 100 most abundant OTUs as follows:

$$252 \quad deviation (\%) = \left(\frac{\bar{X}_{WM}}{\bar{X}_T} \times 100 \right) - 100$$

253 where \bar{X}_{WM} is the mean relative abundance of a OTU in a specific water mass and \bar{X}_T is the
254 mean relative abundance of this OTU in all the samples.

255

256 **RESULTS**

257 The sequencing effort yielded on average $18,111 \pm 14,869$ reads per sample, and ranged
258 from 2,083 to 62,100 pyrotags among the 45 samples (Table 1). For all samples combined, we
259 identified a total of 49,517 unique pyrotag sequences. The pyrotag length averaged 62.51 ± 3.47
260 bp, varying from 51 to 165 bp. On average, the unique V6 pyrotags (i.e., present in only one out
261 of the 45 samples analyzed at an abundance >1) accounted for $14 \pm 3\%$ of the total number of
262 pyrotags in each sample. On average each sample had $2,249 \pm 1,529$ unique bacterial sequences

263 representing nearly 835 ± 421 OTUs (Operational Taxonomic Units) at the 3% difference level.
264 The non-parametric Chao1 and ACE estimate predicted an average number per sample of 1,416
265 ± 787 and $1,733 \pm 1,220$ OTUs, respectively. The rarefaction curves (Fig. S2) indicate that,
266 despite obtaining on average more than 18,000 pyrotags and 10,700 OTUs identified as Bacteria,
267 our sampling of bacterial richness was not complete.

268 To examine another aspect of diversity, the Gini's index of evenness was calculated for
269 each OTU except the singletons (Fig. S3). Most of the OTUs were highly unevenly distributed
270 (Gini > 0.5) comprising both abundant and rare OTUs. The OTUs from subsurface samples
271 exhibited a higher evenness than the OTUs from meso- and bathypelagic samples, indicating that
272 OTUs from subsurface were more equally distributed among samples than OTUs from deeper
273 layers.

274 The 100 and 1,000 most abundant OTUs represented on average $80 \pm 3\%$ and $96 \pm 1\%$,
275 respectively, of the total OTU abundance in the individual samples with no significant difference
276 among the different depth layers or water masses (Fig. 2). Significant differences between depth
277 layers were only observed in the relative contribution of the 5 most abundant OTUs (Kruskal-
278 Wallis test, $H = 7.01$, $p = 0.03$; Fig. 2) representing between 37% and 47% of total OTU
279 abundance. The 5 most abundant OTUs and the 6 – 100 (34-39%) most abundant OTUs
280 contributed roughly equally to the total OTU abundance (Fig. 2). The rank-frequency distribution
281 of the 1,000 most abundant OTUs indicates that only a few OTUs are very abundant with a long
282 tail of low-abundance OTUs (inset, Fig. 2). The rank-frequency distribution of meso- and
283 bathypelagic communities exhibited a steeper slope (slope of 0.58 ± 0.01 and 0.57 ± 0.01 ,
284 respectively) than that of subsurface (slope of 0.32 ± 0.01) OTUs (slope comparison, Student-t

285 test, $p < 0.001$ for all comparisons). The rank-frequency distributions of OTUs of meso- and
286 bathypelagic waters were not significantly different (Student-t test, $p > 0.05$).

287 Singleton OTUs (i.e., present in only one sample at an absolute abundance of 1)
288 comprised 5,567 OTUs out of the 10,780 distinct OTUs in our analysis. They represented half
289 (52%) of the total number of OTUs. However, they accounted for less than 2% of the total OTUs
290 abundance (Fig. 2) and, they were equally distributed among the water layers.

291 Non-metric Multidimensional Scaling (MDS) based on the relative abundance of all
292 OTUs except singletons was used to discriminate bacterial community composition in the
293 different water masses. Cluster analysis showed that bacterial community composition clustered
294 according to the water masses (Fig. 3). The samples separated into one cluster containing
295 bacterial communities of the subsurface zone, one cluster of the mesopelagic waters (AAIW and
296 tCW/SACW) and two deep-water clusters (NEADW and LDW) at 45% of similarity. Two
297 clusters of deep LSW and mesopelagic NIW bacterial communities were identified at the 55%
298 similarity level. The bacterial communities of bathypelagic waters were less similar to each other
299 than samples from subsurface and intermediate waters (Fig. 3). Bacterial communities from the
300 same water mass but separated by thousands of kilometers (S6 from St.A2-11 and S41 from St.
301 A2-45 belonging to subsurface; S12 from St. A2-19 and S40 from St. A2-45 belonging to
302 tCW/SACW; S42 from St. A2-50 and S17 from St. A2-25 belonging to NEADW) were more
303 similar to each other than communities separated by only a few hundred meters at individual
304 sites (S14 and S21 from St. A2-25; S7 and S10 from St. A2-19) but originating from different
305 water masses (Fig. 3, Table S1). The ANOSIM test showed that the differences between the
306 water mass clusters were significant ($p < 0.05$) except for AAIW and tCW/SACW ($p = 0.062$)
307 and for LSW and NIW ($p = 0.1$; Table S3). For this latter pairwise comparison, the R-value was

308 still high ($R = 1$), and the insignificant difference might be due to the low number of samples for
309 each water mass ($n = 3$ for LSW and $n = 2$ for NIW) allowing only 10 permutations (Table S3).
310 A MDS of the 1,000 most abundant OTUs versus all OTUs excluding the singletons produced
311 the same clustering (data not shown). Including singletons in the MDS analysis, however,
312 resulted in a lack of water mass-specificity of bacterial communities (data not shown). SIMPER
313 analysis indicated that the differences in bacterial community composition between water masses
314 are explained by the combination of abundant and rare OTUs (Dataset S1 in Suppl. Information).

315 The clustering of all pyrotags except the singletons was comparable to the clustering of
316 all OTUs except the singletons (Fig S4a). The clustering of the rare sequences (frequency $<$
317 0.01% of total pyrotag abundance within a sample, Fig S4c) was similar to the clustering of the
318 abundant sequences (frequency $>$ 1% within a sample, Fig. S4b), albeit with a generally lower
319 percentage of similarity. The matrices of the abundant and rare pyrotags were significantly
320 related (Mantel test, $r = 0.68$, $p < 0.001$).

321 The similarity of the bacterial communities of the bathy- and mesopelagic waters
322 decreased rapidly from the northernmost station at 60°N (station 27, Transat-2 cruise) to $\approx 50^{\circ}\text{N}$
323 and remained fairly constant thereafter towards the equator (Fig. 4). Besides this pronounced
324 latitudinal trend in similarity in the northern part of the North Atlantic, a pronounced
325 stratification of the bacterial communities was detected (Fig. S5). In the northern part of the
326 North Atlantic, the meso- and bathypelagic bacterial communities were more similar (47.4%)
327 than in the southern part of the North Atlantic (37.7%) indicating an increasing stratification of
328 bacterial communities with decreasing latitude (Fig. S5).

329 The relationship between bacterial assemblage structure (based on the relative abundance
330 of all OTUs), environmental factors and the bacterial activity parameters was assessed by

331 correlating the three distance matrices with a Mantel test. The bacterial assemblage structure
332 correlated with the environmental factors ($r = 0.57$, $p = 0.0001$) but not with bacterial activity
333 parameters ($r = 0.06$, $p = 0.072$). The potential link of environmental factors with bacterial
334 community structure was analyzed by the ordination technique of canonical correspondence
335 analysis (CCA). The CCA indicated that samples clearly clustered according to the water masses
336 (Fig. 5a). Depth and latitude emerged as highly significant explanatory variables, separating
337 samples along the first and the second axes, respectively (Fig. 5a). When depth and latitude were
338 removed from the analysis (Fig. 5b), O_2 concentration, temperature and DOC clearly separated
339 subsurface and bathypelagic samples along the first axis. DON concentration and salinity
340 appeared to be key factors for determining subsurface bacterial assemblage structure. When
341 CCA was applied to bathypelagic samples (Fig. 5c), depth and temperature appeared to be
342 significant explanatory variables, separating bathypelagic samples along the first axis, while
343 DOC and O_2 concentrations separated samples along the second axis. The combination of depth,
344 temperature, salinity, DOC and O_2 concentrations explained 67% of the total variance in the
345 relative abundance of the 1,000 most abundant OTUs in bathypelagic samples. When potential
346 density was used in the analysis instead of depth, the distribution of the bathypelagic samples in
347 the CCA analysis was similar. When CCA was applied to mesopelagic samples (Fig. 5d), the O_2
348 concentration and AOU (apparent oxygen utilization) separated samples along the first axis,
349 while depth and DOC concentration separated samples along the second axis. The combination
350 of these parameters explained about 55% of the total variance in the relative abundance of the
351 1,000 most abundant OTUs in mesopelagic samples.

352

353 **Phylogenetic affiliation of North Atlantic deep-water bacterial communities.**

354 Among the 1,000 most abundant OTUs, *Proteobacteria* were, overall, the most abundant
355 phylum (Fig. 6a), representing $84 \pm 8\%$ of the 1,000 most abundant OTUs. The bathypelagic
356 zone exhibited the highest proportion of unassigned bacteria and a higher evenness than the
357 overlying waters. *Deferribacteres* and, to a lesser extent, *Verrucomicrobia* increased in relative
358 abundance with depth, and contributed 2.5% and 3.9%, respectively, to the bacterial abundance
359 in the bathypelagic zone. *Chloroflexi* contributed to total bacterial abundance 5-fold more in
360 bathypelagic zone (0.25%) than in subsurface (0.05%). In contrast, *Cyanobacteria* decreased
361 with depth from 1.7% of total bacterial abundance in the subsurface layer to 0.2% in the
362 bathypelagic zone (Fig. 6a).

363 Within *Proteobacteria*, *Alphaproteobacteria*, mostly composed of the SAR11 cluster
364 (data not shown), was the most abundant class and accounted for 47% and 68% of the 1,000
365 most abundant proteobacterial OTUs in the bathypelagic and subsurface waters, respectively
366 (Fig. 6b). As at the phylum level, the evenness increased with depth at the class level, and was
367 higher in the bathypelagic zone than in the subsurface and mesopelagic zones. *Gamma-*, *Delta-*
368 and *Betaproteobacteria* increased in relative abundance with depth, and represented 25%, 5%
369 and 5%, respectively, of *Proteobacteria* in the bathypelagic waters.

370 Within *Gammaproteobacteria*, unassigned *Gammaproteobacteria* comprised the major
371 fraction amounting to 83% of the total *Gammaproteobacteria* in the bathypelagic and to 91% in
372 the subsurface waters (Fig. 6c). Also at the order level, evenness increased with depth and some
373 groups were found to be specific to a specific water layer. For example, higher proportions of
374 *Alteromonadales* (7%) and, to a lesser extent, *Oceanospirillales* (4%), *Enterobacteriales* (2%)
375 and *Pseudomonadales* (1.6%) were found in the bathypelagic than in the subsurface zone (Fig.
376 6c). In contrast, *Chromatiales* were more restricted to subsurface (4%) than deep layers (1%).

377 Analysis of the taxonomic composition of the singletons revealed that they were as
378 diverse as the abundant OTUs (Fig. 7). Most of the singletons belonged to the *Proteobacteria*
379 (61%) but 11% were unassigned (Fig. 7a). Within *Proteobacteria*, *Alpha-* (38%) and
380 *Gammaproteobacteria* (29%) dominated and 16% of the gammaproteobacterial OTUs remained
381 unassigned (Fig. 7b). Overall, the phylogenetic composition of the singleton community was
382 similar among all three water layers and similar to the bacterial assemblage structure of the 1,000
383 most abundant OTUs at the phylum (Mantel test, $r = 0.56$, $p = 0.001$) and the class level within
384 the *Proteobacteria* (Mantel test, $r = 0.33$, $p = 0.001$).

385 The deviation (in %) from the mean relative abundance in all the samples of the 100 most
386 abundant OTUs (accounting for $79 \pm 8\%$ of the OTUs abundance over all the water masses) was
387 calculated for each water mass (Fig. 8). Lower abundance OTUs exhibit higher water mass
388 specificity than the more abundant OTUs. OTUs specific for LSW included members of the
389 SAR324 clade (belonging to the *Deltaproteobacteria*; OTU #3, Fig. 8 and Table S4) which
390 accounted for 7% of the 100 most abundant OTUs, members of the SAR406 clade (belonging to
391 *Fibrobacteres*, OTUs #30, 40 and 60) which showed the greatest variability observed among the
392 100 most abundant OTUs, members of the *Gammaproteobacteria* (OTUs #77, 89),
393 *Gemmatimonadetes* (OTU #73) and *Actinobacteria* (OTU #86). OTUs specific for the NEADW
394 included members of the *Alphaproteobacteria* (OTUs #11, 16, 24, 65 and 87), the
395 *Betaproteobacteria* (OTU #23), the *Gammaproteobacteria* (OTUs #35, 41, 52, 66, 74 and 100),
396 the *Deltaproteobacteria* (OTUs #75, 81, 91), the *Fibrobacteres* (members of the SAR406 clade,
397 OTUs #25 and 98) and the *Verrucomicrobiales* (OTU #46) (Fig. 8 and Table S4). Members of
398 the *Chloroflexi*-type SAR202 cluster (OTUs #39, 69) were generally specific for deep waters
399 (NEADW and LSW). A large number of OTUs specific for mesopelagic waters were affiliated to

400 unassigned *Alphaproteobacteria* (OTUs #12, 53, 71, 83 and 90) and one OTU to the
401 *Verrucomicrobiales* phylum (OTU #20) (Fig. 8 and Table S4). Surface-specific OTUs were
402 mainly members of unassigned *Alphaproteobacteria* (OTUs #18, 32, 38, 48, 61, 70) and
403 *Gammaproteobacteria* (OTUs # 50, 67, 85) and one OTU from the *Actinobacteria* (OTU #99).
404 Members of the SAR11 clade (OTUs #1, 2, and 96) exhibited a ubiquitous distribution, albeit
405 they were relatively less abundant in deep-water masses (NEADW, core NEADW and LSW)
406 than in subsurface and mesopelagic waters (250 – 500m and AAIW) (Fig. 8 and Table S4). The
407 SAR11 clade contributed about 37% to the relative abundance of the 100 most abundant OTUs.

408

409 **DISCUSSION**

410 The pyrosequencing approach allowed a deep sampling of bacterial communities in North
411 Atlantic waters. The analyses of 45 samples, originating from 10 stations along a 8,000 km
412 north-to-south transect provide an exhaustive description of the distribution of bacterial
413 communities in the major deep-water masses of the North Atlantic.

414 We found water mass-specific clustering of bacterial communities throughout the major
415 North Atlantic water masses. These differences in the phylogenetic composition of the bacterial
416 community between water masses are not only due to the most abundant OTUs, but the less
417 abundant OTUs including the rare ones (but not the singletons) are also responsible for the water
418 mass-specificity of the bacterial community composition. This implies that the less abundant
419 bacterial populations exhibit biogeographical traits while the most abundant ones are more
420 ubiquitously distributed. Previous studies suggested that the rare biosphere should exhibit a high
421 rate of dispersal (Fenchel & Finlay 2004; Finlay 2002) and might act as a “seed-bank” of micro-
422 organisms which might become abundant in case of environmental changes (Palacios *et al.* 2008;

423 Pedros-Alio 2006). Kirchman *et al.* (2010), however, argued against the “seed-bank” hypothesis
424 as rare phylotypes of the winter bacterial community remained rare also in the summer
425 community in the Arctic Ocean. The distribution patterns observed for rare OTUs in the North
426 Atlantic Ocean indicate that the rare bacterial biosphere contributes to the water mass-specificity
427 of bacterial communities. Hence, the rare biosphere is most likely not maintained by stochastic
428 immigration but appears to be a water mass property as also shown for the Arctic Ocean (Galand
429 *et al.* 2010). A ubiquitous distribution of members of the rare bacterial biosphere, as previously
430 suggested (Pedros-Alio 2006), was not found in the deep-waters of the Atlantic challenging the
431 idea that “everything is everywhere” (Baas Becking 1934).

432 The singletons, *i.e.*, the OTUs present only once in all the samples, are included in the
433 rare bacterial biosphere (Sogin *et al.* 2006). Before speculating on the potential ecological role of
434 the rare bacterial biosphere and its origin, we need to address the question whether the presence
435 of singletons generated by the pyrosequencing approach are fact or artifact. Random sequencing
436 errors and miscalled bases could potentially be an explanation for the high number of singleton
437 sequences (Gomez-Alvarez *et al.* 2009; Quince *et al.* 2009; Reeder & Knight 2009) and could
438 inflate actual diversity estimates (Kunin *et al.* 2009). Increased sampling effort leads to a greater
439 probability that OTUs from a given template will include variant sequences and therefore inflate
440 the number of observed singletons. However, the frequency of variant sequences will be a
441 function of the relative abundance of a unique starting template and the number of generated
442 OTUs for the entire community. Sequences that correspond to high frequency templates are more
443 likely to produce variants. A systematic and stringent trimming procedure was used in this study
444 to remove low quality sequences and reads that did not represent the targeted region. This
445 procedure results in a per-base error rate of 0.2-0.4% (Huse *et al.* 2007). Moreover, the newly

446 developed clustering method applied in this study removes spurious OTUs produced by
447 pyrosequencing errors and minimizes the inflation of OTUs with sequencing effort (Huse *et al.*
448 2010). In our study, the singletons represent only 2% of the total OTU abundance in each depth
449 zone of the North Atlantic. No clear clustering according to water masses was obtained when the
450 singletons were included in the MDS analysis, while the bacterial community structure using all
451 the OTUs except the singletons exhibits a water-mass specific clustering. As the singletons have
452 the same phylogenetic composition as the 1,000 most abundant OTUs, some of the singletons
453 might be artifacts resulting from noise in high-throughput pyrosequencing of the most abundant
454 OTUs (Reeder & Knight 2009).

455

456 **Biogeography of bacterial communities in the thermohaline ocean circulation of the North** 457 **Atlantic**

458 Distance, latitudinal gradients and area have been shown to influence bacterial
459 community composition in lakes and the ocean (Fuhrman *et al.* 2008; Hewson *et al.* 2006; Reche
460 *et al.* 2005). Recent phylogenetic surveys revealed a pronounced stratification among specific
461 groups of planktonic Bacteria (DeLong 2005; Galand *et al.* 2010; Hewson *et al.* 2006; Kirchman
462 *et al.* 2010; Martin-Cuadrado *et al.* 2007; Suzuki *et al.* 2004; Treusch *et al.* 2009) and Archaea
463 (Agogu e *et al.* 2008; Galand *et al.* 2009b; Garcia-Martinez & Rodriguez-Valera 2000). In our
464 study, the similarity in bacterial community composition decreases rapidly in the meso- and
465 bathypelagic waters from 60°N to 50°N and remains fairly stable thereafter. Moreover, the
466 similarity in bacterial community composition between meso- and bathypelagic waters was
467 higher in the northern than in the southern part of the transect. This reflects the large scale deep-
468 water formation in the northern North Atlantic leading to a more uniform deep-water bacterial

469 community in the generally younger deep waters in the northern North Atlantic also exhibiting
470 smaller differences in physico-chemical parameters between meso- and bathypelagic waters than
471 further south towards the (sub)tropical Atlantic. Further south, distance was influencing bacterial
472 community composition much less than water mass identity in the (sub)tropical Atlantic Ocean.

473 Analysis of the affiliation of the 100 most abundant OTUs revealed obvious water mass-
474 specific signatures of bacterial community structure. Due to their distinct temperature and
475 salinity characteristics, water masses might act as presumed dispersal barriers for
476 bacterioplankton and hence, might limit immigration of bacterial phylotypes (Aristegui *et al.*
477 2009) from adjacent water masses. In the bathypelagic realm, depth and temperature were the
478 main factors determining the composition of bacterial communities and discriminating samples
479 from different water masses. Salinity, temperature and consequently density act as potential
480 oceanographic barriers separating water masses and their inhabiting bacterial communities
481 (Pommier *et al.* 2007) generating bio-oceanographic islands with specific signatures of bacterial
482 community composition such as shown most pronouncedly for North East Atlantic Deep Water
483 and Labrador Sea Water. Besides water mass identity and latitude, the specific environmental
484 properties of the water masses, such as the concentrations of DOC and O₂, and AOU determine
485 the bacterial community composition in the North Atlantic Ocean.

486 In contrast to our current perception of the deep ocean as a rather low diversity
487 environment, bacterial community richness and evenness in the bathypelagic waters of the North
488 Atlantic are as high and as variable as subsurface and mesopelagic waters. This observation is
489 consistent with previous reports on bacterial diversity of the North Pacific and Atlantic (Hewson
490 *et al.* 2006) and in the eastern Mediterranean Sea (Moeseneder *et al.* 2001) using fingerprinting
491 techniques. This reported heterogeneity in deep bacterial assemblages contrasts the very slow

492 assemblage growth rates estimated to be $0.061 \pm 0.008 \text{ d}^{-1}$ in the deep Pacific (Aristegui *et al.*
493 2009) and deep-water movement (1.5 cm s^{-1}) (van Aken 2007). The heterogeneity in deep-water
494 bacterial community composition has been interpreted to result from episodic input of organic
495 matter from surface waters and patchiness (Hewson *et al.* 2006). However, it appears that
496 microbial life in the dark ocean is likely more dependent on slowly sinking or buoyant, laterally
497 advected suspended particles than hitherto assumed (Bochdansky *et al.* 2010) which might
498 generate the water mass-specific biogeochemical conditions leading ultimately to water mass-
499 specific bacterial assemblages (Baltar *et al.* 2009).

500

501 **Vertical distribution of bacterial phylotypes**

502 As found in previous studies on deep-sea bacterial diversity (DeLong *et al.* 2006;
503 Fuhrman & Davis 1997; Lopez-Garcia *et al.* 2001; Pham *et al.* 2008), *Proteobacteria*, mostly
504 from the alpha subdivision, dominate the bacterial community. Members of the
505 alphaproteobacterial clade SAR11, ubiquitously present in the ocean (DeLong *et al.* 2006; Field
506 *et al.* 1997; Giovannoni *et al.* 1990; Morris *et al.* 2002), decreased in relative abundance with
507 depth.

508 The relative abundance of *Gammaproteobacteria*, however, increased with depth as
509 reported previously for the North Atlantic (Lauro & Bartlett 2008; Sogin *et al.* 2006) and
510 Antarctic Polar Front (Lopez-Garcia *et al.* 2001). Within *Gammaproteobacteria*, members of the
511 order *Alteromonadales* are abundant in bathypelagic waters. Several psychropiezophilic (cold
512 and pressure-loving) bacterial isolates such as *Moritella sp.* PE36, *Psychromonas sp.* CNPT3 and
513 *Shewanella sp.* KT99 are belonging to this order (DeLong *et al.* 1997; Lauro *et al.* 2007). We
514 also found members of the *Oceanospirillales* more abundant in the bathypelagic North Atlantic

515 waters than in the subsurface and mesopelagic layers. Members of this order are also known to
516 be symbionts of the deep-sea worm *Osedax sp.* (Goffredi *et al.* 2007; Rouse *et al.* 2009).
517 *Betaproteobacteria* also increased in relative abundance with depth. OTUs affiliated to this class
518 are closely related to endosymbionts of bivalves found at hydrothermal vents (Kimura *et al.*
519 2003). Their relatively high abundance in the free-living mode in bathypelagic waters,
520 particularly in the North East Atlantic Deep Water (NEADW) might indicate their spreading
521 from hydrothermal vents and/or seafloor as the NEADW flows mainly along the eastern slope of
522 the mid-Atlantic ridge. Free-living *Betaproteobacteria* are common in freshwaters (Kirchman *et*
523 *al.* 2005) but not abundant in the bathypelagic realm. However, metagenomic analysis from
524 deep-sea methane vents have reported *Betaproteobacteria*-related phylotypes (Pernthaler *et al.*
525 2008), suggesting a potential niche for these organisms within methane-rich deep marine
526 environments. In the North Pacific Ocean, Brown *et al.* (2009) recently reported an increasing
527 relative abundance of *Betaproteobacteria* V9 pyrotags at 800m and 4400m depth. The
528 bathypelagic bacterial community of the North Atlantic was also enriched in
529 *Deltaproteobacteria*, as previously shown for the deep Arctic Ocean as well (Galand *et al.*
530 2010)) and for Station ALOHA in the North Pacific Subtropical Gyre (DeLong *et al.* 2006).

531 The comparison of the phylogenetic composition of the 1,000 most abundant OTUs
532 reveals an increase of OTUs richness and evenness with depth. Thus, the bacterial community of
533 the North Atlantic is more diverse in the bathypelagic realm than that at the base of the euphotic
534 layer. The composition of the 100 most abundant OTUs indicates distinct water mass-specific
535 OTUs, especially in deep waters. In meso- and bathypelagic waters, the *Deltaproteobacteria*
536 were dominated by the SAR324 cluster (Wright *et al.* 1997), a typical deep-water clade (DeLong
537 *et al.* 2006; Lopez-Garcia *et al.* 2001; Pham *et al.* 2008; Zaballos *et al.* 2006). The SAR406

538 cluster (Gordon & Giovannoni 1996) previously detected in various oceanic provinces
539 (Gallagher *et al.* 2004; Pham *et al.* 2008) is another abundant clade of the deep Atlantic ocean,
540 specific to the LSW. *Chloroflexi*-type SAR202 cluster, described as highly abundant in the
541 bathypelagic subtropical North Atlantic (Morris *et al.* 2004; Varela *et al.* 2008a; Wright *et al.*
542 1997) was found to be a specific member of the NEADW.

543

544 **Concluding remarks**

545 By applying a high-throughput pyrosequencing strategy, we achieved a deep coverage of
546 the bacterial populations in the deep-water masses of the North Atlantic. The bacterial
547 assemblages clearly clustered according to the distinct water masses. The low abundance OTUs
548 were as important for the observed water mass-specificity of bacterial community composition as
549 the more abundant OTUs. Density differences separate water masses and their inhabiting
550 bacterial communities, generating bio-oceanographic islands with specific signatures of bacterial
551 community composition such as shown most pronouncedly for the deep waters. The deep
552 bacterial assemblages exhibit a higher richness and evenness than bacterial assemblages at the
553 base of the euphotic layer suggesting that the bathypelagic waters might offer a more
554 heterogeneous environment for microbial life than hitherto assumed.

555

556 **Acknowledgements**

557 We acknowledge the help of H.M. van Aken for the characterization of the water masses,
558 J. M. Arrieta for collecting and extracting the samples of the TRANSAT-1 cruise, M. Brink and
559 D. de Corte for extracting the samples of ARCHIMEDES-2 cruise, F. Baltar for the dataset on
560 ectoenzymatic activity, D.M Welch and S.M. Huse for the dataset on OTUs sequences and T.

561 Reinthaler for providing the parameters datasets of Transat and Archimedes cruises. The captain
562 and crew of RV Pelagia provided excellent service at sea.

563 - Author contribution. G.J.H. and M.S. sampling scheme and sample analyses, H.A., D.L. and
564 P.N. analyzed the data, G.J.H., P.N. and M.S. contributed the reagents/materials/analysis tools,
565 H.A., D.L. and G.J.H wrote the paper.

566 - Funding. This research was supported by two Marie Curie Fellowships of the European
567 Community to D.L. and H.A., by the Alfred P. Sloan Foundation's ICoMM field project, the W.
568 M. Keck Foundation and a subcontract from the Woods Hole Center for Oceans and Human
569 Health from the National Institutes of Health and the National Science Foundation (NIH_NIEHS
570 1 P50 ES012742-01 and NSF_OCE 0430724-J. Stegeman PI to M.L.S.). Shiptime was provided
571 through grants of the Earth and Life Science Division of the Dutch Science Foundation (ALW-
572 NWO) (TRANSAT and ARCHIMEDES projects) to G.J.H.

573 - Competing interests. The authors have declared that no competing interests exist.

574

575 REFERENCES

576

577 Agogué H, Brink M, Dinasquet J, Herndl GJ (2008) Major gradients in putatively nitrifying and
578 non-nitrifying Archaea in the deep North Atlantic. *Nature*, **456**, 788-791.

579 Andersson AF, Riemann L, Bertilsson S (2009) Pyrosequencing reveals contrasting seasonal
580 dynamics of taxa within Baltic Sea bacterioplankton communities. *ISME Journal*, **4**, 171-
581 181.

582 Aristegui J, Gasol JM, Duarte CM, Herndl GJ (2009) Microbial oceanography of the dark
583 ocean's pelagic realm. *Limnology and Oceanography*, **54**, 1501-1529.

584 Azam F, Fenchel T, Field JG, *et al.* (1983) The Ecological Role of Water-Column Microbes in
585 the Sea. *Marine Ecology Progress Series*, **10**, 257-263.

586 Baas Becking LGM (1934) *Geobiologie of inleiding tot de milieukunde*, The Hague, the
587 Netherlands.

588 Baltar F, Aristegui J, Gasol JM, Sintes E, Herndl GJ (2009) Evidence of prokaryotic metabolism
589 on suspended particulate organic matter in the dark waters of the subtropical North
590 Atlantic. *Limnology and Oceanography*, **54**, 182-193.

591 Bochdansky AB, van Aken HM, Herndl GJ (2010) Role of macroscopic particles in deep-sea
592 oxygen consumption. *Proceedings of the National Academy of Sciences, USA*, **107**, 8287-
593 8291.

594 Brown MV, Philip GK, Bunge JA, *et al.* (2009) Microbial community structure in the North
595 Pacific ocean. *ISME Journal*, **3**, 1374-1386.

596 Bunge JA, Woodard L, Connolly S (2010) CatchAll: Parametric and nonparametric estimation of
597 species richness and population size. *Manuscript in preparation*.

598 Clarke KR, Warwick RM (2001) Change in marine communities: an approach to statistical
599 analysis and interpretation. In: *PRIMER-E Ltd*, Plymouth, UK.

600 DeLong EF (2005) Microbial community genomics in the ocean. *Nature Reviews: Microbiology*,
601 **3**, 459-469.

602 DeLong EF, Franks DG, Yayanos AA (1997) Evolutionary Relationships of Cultivated
603 Psychrophilic and Barophilic Deep-Sea Bacteria. *Applied and Environmental*
604 *Microbiology*, **63**, 2105-2108.

605 DeLong EF, Preston CM, Mincer T, *et al.* (2006) Community genomics among stratified
606 microbial assemblages in the ocean's interior. *Science* **311**, 496-503.

607 Fenchel T, Finlay BJ (2004) The ubiquity of small species: Patterns of local and global diversity.
608 *BioScience*, **54**.

609 Field KG, Gordon D, Wright T, *et al.* (1997) Diversity and depth-specific distribution of SAR11
610 cluster rRNA genes from marine planktonic bacteria. *Applied and Environmental*
611 *Microbiology*, **63**, 63-70.

612 Finlay BJ (2002) Global dispersal of free-living microbial eucaryote species. *Science*, **296**.

613 Fuhrman JA, Davis AA (1997) Widespread archaea and novel bacteria from the deep sea as
614 shown by 16S rRNA gene sequences. *Marine Ecology-Progress Series*, **150**, 275-285.

615 Fuhrman JA, Sleeter TD, Carlson CA, Proctor LM (1989) Dominance of bacterial biomass in the
616 Sargasso Sea and its ecological implications. *Marine Ecology Progress Series*, **57**, 207-
617 217.

618 Fuhrman JA, Steele JA, Hewson I, *et al.* (2008) A latitudinal diversity gradient in planktonic
619 marine bacteria. *Proceedings of the National Academy of Sciences*, **105**, 7774-7778.

620 Galand PE, Casamayor EO, Kirchman DL, Lovejoy C (2009a) Ecology of the rare microbial
621 biosphere of the Arctic Ocean. *Proceedings of the National Academy of Sciences, USA*,
622 **106**, 22427-22432.

623 Galand PE, Casamayor EO, Kirchman DL, Potvin M, Lovejoy C (2009b) Unique archaeal
624 assemblages in the Arctic Ocean unveiled by massively parallel tag sequencing. *ISME*
625 *Journal*, **3**, 860-869.

626 Galand PE, Potvin M, Casamayor EO, Lovejoy C (2010) Hydrography shapes bacterial
627 biogeography of the deep Arctic Ocean. *ISME Journal*, **4**, 564-576.

628 Gallagher JM, Carton MW, Eardly DF, Patching JW (2004) Spatio-temporal variability and
629 diversity of water column prokaryotic communities in the eastern North Atlantic. *FEMS*
630 *Microbiology Ecology* **47**, 249-262.

631 Garcia-Martinez J, Rodriguez-Valera F (2000) Microdiversity in uncultured marine prokaryotes:
632 the SAR11 cluster and the marine Archaea of Group I. *Molecular Ecology*, **9**, 935-948.

633 Gilbert JA, Field D, Swift P, *et al.* (2009) The seasonal structure of microbial communities in the
634 Western English Channel. *Environmental Microbiology*, **11**, 3132-3139.

635 Giovannoni SJ, Britschgi TB, Moyer CL, Field KG (1990) Genetic Diversity in Sargasso Sea
636 Bacterioplankton. *Nature*, **345**, 60-63.

637 Goffredi SK, Johnson SB, Vrijenhoek RC (2007) Genetic Diversity and Potential Function of
638 Microbial Symbionts Associated with Newly Discovered Species of Osedax Polychaete
639 Worms. *Applied and Environmental Microbiology*, **73**, 2314-2323.

640 Gomez-Alvarez V, Teal TK, Schmidt TM (2009) Systematic artifacts in metagenomes from
641 complex microbial communities. *ISME Journal*, **11**, 1314-1317.

642 Gordon DA, Giovannoni SJ (1996) Detection of stratified microbial populations related to
643 Chlorobium and Fibrobacter species in the Atlantic and Pacific Oceans. *Applied and
644 Environmental Microbiology*, **62**, 1171-1177.

645 Handelsman J (2004) Metagenomics: Application of Genomics to Uncultured Microorganisms.
646 *Microbiology and Molecular Biology Reviews*, **68**, 669-685.

647 Hewson I, Steele JA, Capone DG, Fuhrman JA (2006) Remarkable heterogeneity in meso- and
648 bathypelagic bacterioplankton assemblage composition. *Limnology and Oceanography*,
649 **51**, 1274-1283.

650 Huber JA, Mark Welch D, Morrison HG, *et al.* (2007) Microbial population structures in the
651 deep marine biosphere. *Science*, **318**, 97-100.

652 Huse SM, Dethlefsen L, Huber JA, *et al.* (2008) Exploring Microbial Diversity and Taxonomy
653 Using SSU rRNA Hypervariable Tag Sequencing. *Plos Genetics*, **4**, e10000255.

654 Huse SM, Huber JA, Morrison HG, Sogin ML, Mark Welch D (2007) Accuracy and quality of
655 massively parallel DNA pyrosequencing. *Genome Biology*, **8**, R143.

656 Huse SM, Welch DM, Morrison HG, Sogin ML (2010) Ironing out the wrinkles in the rare
657 biosphere through improved OTU clustering. *Environmental Microbiology*,
658 doi:10.1111/j.1462-2920.2010.02193.x.

659 Karl DM (2002) Nutrient dynamics in the deep blue sea. *Trends in Microbiology*, **10**, 410-418.

660 Kimura H, Higashide Y, Naganuma T (2003) Endosymbiotic microflora of the vestimentiferan
661 tubeworm (*Lamellibrachia sp.*) from a bathyal cold seep. *Marine Biotechnology*, **5**, 593-
662 603.

663 Kirchman DL, Cottrell MT, Lovejoy C (2010) The structure of bacterial communities in the
664 western Arctic Ocean as revealed by pyrosequencing of 16S rRNA genes. *Environmental
665 Microbiology*, **12**, 1132-1143.

666 Kirchman DL, Dittel AI, Malmstrom RR, Cottrell MT (2005) Biogeography of major bacterial
667 groups in the Delaware Estuary. *Limnology and Oceanography*, **50**, 1697-1706.

668 Kruskal JB (1964a) Multidimensional-Scaling by optimizing goodness of fit to a nonmetric
669 hypothesis. *Psychometrika*, **29**, 1-27.

670 Kruskal JB (1964b) Nonmetric Multidimensional Scaling - a numerical method. *Psychometrika*,
671 **29**, 115-129.

672 Kunin V, Engelbrekton A, Ochman H, Hugenholtz P (2009) Wrinkles in the rare biosphere:
673 pyrosequencing errors lead to artificial inflation of diversity estimates. *Environmental
674 Microbiology*, **1**, 118-123.

675 Lauro FM, Bartlett DH (2008) Prokaryotic lifestyles in deep sea habitats. *Extremophiles*, **12**, 15-
676 25.

677 Lauro FM, Chastain RA, Blankenship LE, Yayanos AA, Bartlett DH (2007) The Unique 16S
678 rRNA Genes of Piezophiles Reflect both Phylogeny and Adaptation. *Applied and
679 Environmental Microbiology*, **73**, 838-845.

680 Lopez-Garcia P, Lopez-Lopez A, Moreira D, Rodriguez-Valera F (2001) Diversity of free-living
681 prokaryotes from a deep-sea site at the Antarctic Polar Front. *Fems Microbiology
682 Ecology*, **36**, 193-202.

683 Margulies M, Egholm M, Altman WE, *et al.* (2005) Genome sequencing in microfabricated
684 high-density picolitre reactors. *Nature*, **437**, 376-380.

685 Martin-Cuadrado A-B, Lopez-Garcia P, Alba J-C, *et al.* (2007) Metagenomics of the Deep
686 Mediterranean, a Warm Bathypelagic Habitat. *PLoS ONE*, **2**, e914.

687 Martiny JBH, Bohannan BJM, Brown JH, *et al.* (2006) Microbial biogeography: putting
688 microorganisms on the map. *Nature Reviews: Microbiology*, **4**, 102-112.

689 Moeseneder MM, Winter C, Arrieta JM, Herndl GJ (2001) Terminal-restriction fragment length
690 polymorphism (T-RFLP) screening of a marine archaeal clone library to determine the
691 different phylotypes. *Journal of Microbiol Methods*, **44**, 159-172.

692 Morris RM, Rappe MS, Connon SA, *et al.* (2002) SAR11 clade dominates ocean surface
693 bacterioplankton communities. *Nature*, **420**, 806-810.

694 Morris RM, Rappe MS, Urbach E, Connon SA, Giovannoni SJ (2004) Prevalence of the
695 Chloroflexi-Related SAR202 Bacterioplankton Cluster throughout the Mesopelagic Zone
696 and Deep Ocean. *Applied and Environmental Microbiology*, **70**, 2836-2842.

697 Olsen GJ, Lane DJ, Giovannoni SJ, Pace NR, Stahl DA (1986) Microbial Ecology and
698 Evolution: A Ribosomal RNA Approach. *Annual Review of Microbiology*, **40**, 337-365.

699 Palacios C, Zettler E, Amils R, Amaral-Zettler L (2008) Contrasting microbial community
700 assembly hypotheses: a reconciling tale from the Rio Tinto. *PLoS One*, **3**, e3853.

701 Pedros-Alio C (2006) Marine microbial diversity: can it be determined? *Trends in Microbiology*,
702 **14**, 257-263.

703 Pernthaler A, Dekas AE, Brown CT, *et al.* (2008) Diverse syntrophic partnerships from deep-sea
704 methane vents revealed by direct cell capture and metagenomics. *Proceedings of the
705 National Academy of Sciences, USA*, **105**, 7052-7057.

706 Pham VD, Konstantinidis KT, Palden T, DeLong EF (2008) Phylogenetic analyses of ribosomal
707 DNA-containing bacterioplankton genome fragments from a 4000 m vertical profile in
708 the North Pacific Subtropical Gyre. *Environmental Microbiology*, **10**, 2313-2330.

709 Pommier T, Canback B, Riemann L, *et al.* (2007) Global patterns of diversity and community
710 structure in marine bacterioplankton. *Molecular Ecology*, **16**, 867-880.

711 Pommier T, Pinhassi J, Hagstrom A (2005) Biogeographic analysis of ribosomal RNA clusters
712 from marine bacterioplankton. *Aquatic Microbial Ecology*, **41**, 79-89.

713 Quince C, Lanzen A, Curtis TP, *et al.* (2009) Accurate determination of microbial diversity from
714 454 pyrosequencing data. *Nature Methods*, **6**, 639-641.

715 Reche I, Pulido-Villena E, Morales-Baquero R, Casamayor EO (2005) Does ecosystem size
716 determine aquatic bacterial richness? *Ecology*, **86**, 1715-1722.

717 Reeder J, Knight R (2009) The 'rare biosphere': a reality check. *Nature Methods*, **6**, 636-637.

718 Rouse G, Wilson N, Goffredi S, *et al.* (2009) Spawning and development in Osedax boneworms
719 (Siboglinidae, Annelida). *Marine Biology*, **156**, 395-405.

720 Sloan WT, Lunn M, Woodcock S, *et al.* (2006) Quantifying the roles of immigration and chance
721 in shaping prokaryote community structure. *Environmental Microbiology*, **8**, 732-740.

722 Sogin ML, Morrison HG, Huber JA, *et al.* (2006) Microbial diversity in the deep sea and the
723 underexplored "rare biosphere". *Proceedings of the National Academy of Sciences, USA*,
724 **103**, 12115-12120.

725 Suzuki MT, Preston CM, Beja O, *et al.* (2004) Phylogenetic screening of ribosomal RNA gene-
726 containing clones in bacterial artificial chromosome (BAC) libraries from different
727 depths in Monterey Bay. *Microbial Ecology*, **48**, 473-488.

728 Ter Braak CJ, Verdonschot PF (1995) Canonical correspondence analysis and related
729 multivariate methods in aquatic ecology. *Aquatic Sciences*, **57**, 255-289.
730 Ter Braak CJF (1989) CANOCO - an extension of DECORANA to analyze species-environment
731 relationships. *Hydrobiologia*, **184**, 169-170.
732 Tomczak M, Godfrey JS (2003) *Regional Oceanography: An Introduction*, 2nd edn. Daya
733 Publishing House, Delhi.
734 Treusch AH, Vergin KL, Finlay LA, *et al.* (2009) Seasonality and vertical structure of microbial
735 communities in an ocean gyre. *ISME Journal*, **3**, 1148-1163.
736 van Aken HM (2000a) The hydrography of the mid-latitude northeast Atlantic Ocean: I: The
737 deep water masses. *Deep Sea Research Part I*, **47**, 757-788.
738 van Aken HM (2000b) The hydrography of the mid-latitude Northeast Atlantic Ocean: II: The
739 intermediate water masses. *Deep Sea Research Part I*, **47**, 789-824.
740 van Aken HM (2007) *The oceanic thermohaline circulation*, Springer, New York.
741 Varela MM, van Aken HM, Herndl GJ (2008a) Abundance and activity of Chloroflexi-type
742 SAR202 bacterioplankton in the meso- and bathypelagic waters of the (sub)tropical
743 Atlantic. *Environmental Microbiology*, **10**, 1903-1911.
744 Varela MM, van Aken HM, Sintès E, Herndl GJ (2008b) Latitudinal trends of Crenarchaeota and
745 Bacteria in the meso- and bathypelagic water masses of the Eastern North Atlantic.
746 *Environmental Microbiology*, **10**, 110-124.
747 Wittebolle L, Marzorati M, Clement L, *et al.* (2009) Initial community evenness favours
748 functionality under selective stress. *Nature*, **458**, 623-626.
749 Wright TD, Vergin KL, Boyd PW, Giovannoni SJ (1997) A novel delta-subdivision
750 proteobacterial lineage from the lower ocean surface layer. *Applied and Environmental*
751 *Microbiology*, **63**, 1441-1448.
752 Zaballos M, Lopez-Lopez A, Ovreas L, *et al.* (2006) Comparison of prokaryotic diversity at
753 offshore oceanic locations reveals a different microbiota in the Mediterranean Sea. *FEMS*
754 *Microbiology Ecology*, **56**, 389-405.
755

756 **Figure captions**

757 **Figure 1.** Location of the stations where samples for pyrosequencing were taken during the
758 Transat-1, Transat-2 and Archimedes-2 cruises in the North Atlantic. Characteristics of the
759 samples are given in Table S1.

760 **Figure 2.** Depth distribution of the 5, 6 – 100 and 101 – 1,000 most abundant OTUs and the
761 singletons. Inset: Rank-frequency distribution of the 1,000 most abundant OTUs.

762 **Figure 3.** Non-metric multidimensional analysis based on relative abundance of all OTUs except
763 the singletons. Individual samples were affiliated to their respective water-mass. Superimposed
764 circles represent clusters of samples at similarity values of 45 and 55% (Bray-Curtis similarity).
765 Characteristics of the samples are indicated in Table S1. The final solution was based on 25
766 iterations with a final stress of 0.12.

767 **Figure 4.** Similarity in relative abundance of all OTUs except the singletons (in %, calculated
768 through SIMPER analysis) between each station and the northernmost station of the transect
769 (station 27, Transat-2) within bathy- and mesopelagic water layers.

770 **Figure 5.** Canonical correspondence analysis of the relative abundance of the 1,000 most
771 abundant OTUs (a) for all samples, (b) for all samples without depth and latitude as explanatory
772 variables, (c) for bathypelagic samples and (d) for mesopelagic samples. Monte Carlo
773 permutation tests for the first and all axes were highly significant for all the four CCA analyses
774 ($p < 0.002$). Abbreviations of the environmental and bacteria-related variables: lat, latitude; O₂,
775 oxygen concentration; AOU, apparent oxygen utilization; DOC, dissolved organic carbon; DON,
776 dissolved organic nitrogen; Sal, salinity; NH₄, ammonium concentration.

777 **Figure 6.** Relative abundance and affiliation of the 1000 most abundant bacterial OTUs of each
778 zone of the Atlantic Ocean (subsurface n=6, mesopelagic n=20 and bathypelagic n=19). (a) on

779 the phylum level, (b) the class level within *Proteobacteria*, (c) the order level within
780 *Gammaproteobacteria*.

781 **Figure 7.** Relative abundance and affiliation of the singletons of each zone of the Atlantic Ocean
782 (subsurface n=6, mesopelagic n=20 and bathypelagic n=19). (a) on the phylum level, and (b) the
783 class level within *Proteobacteria*.

784 **Figure 8.** Deviation (in %) from the mean relative abundance of the 100 most abundant OTUs
785 for all the samples for the different water masses.

786

787 **Tables**788 **Table 1.** Sequencing information and diversity estimates for the 45 samples of the North Atlantic

789 Ocean obtained by pyrosequencing.

| | Average per sample | Standard deviation | Range |
|---|---------------------------|---------------------------|--------------|
| Pyrotag length (bp) | 62.51 | ± 3.47 | 51 - 165 |
| Total number of pyrotags | 18111 | ± 14869 | 2083 - 62100 |
| Total unique pyrotags | 2249 | ± 1529 | 479 - 7241 |
| % of total unique pyrotags | 14 | ± 3 | 6 - 23 |
| Total OTUs at 3% difference | 835 | ± 421 | 245 - 2063 |
| Chao1 estimator of richness at 3% difference | 1416 | ± 787 | 431 - 4032 |
| ACE estimator of richness at 3% difference | 1733 | ± 1220 | 552 - 7453 |

790

791

792

793

794

795

796

797

798

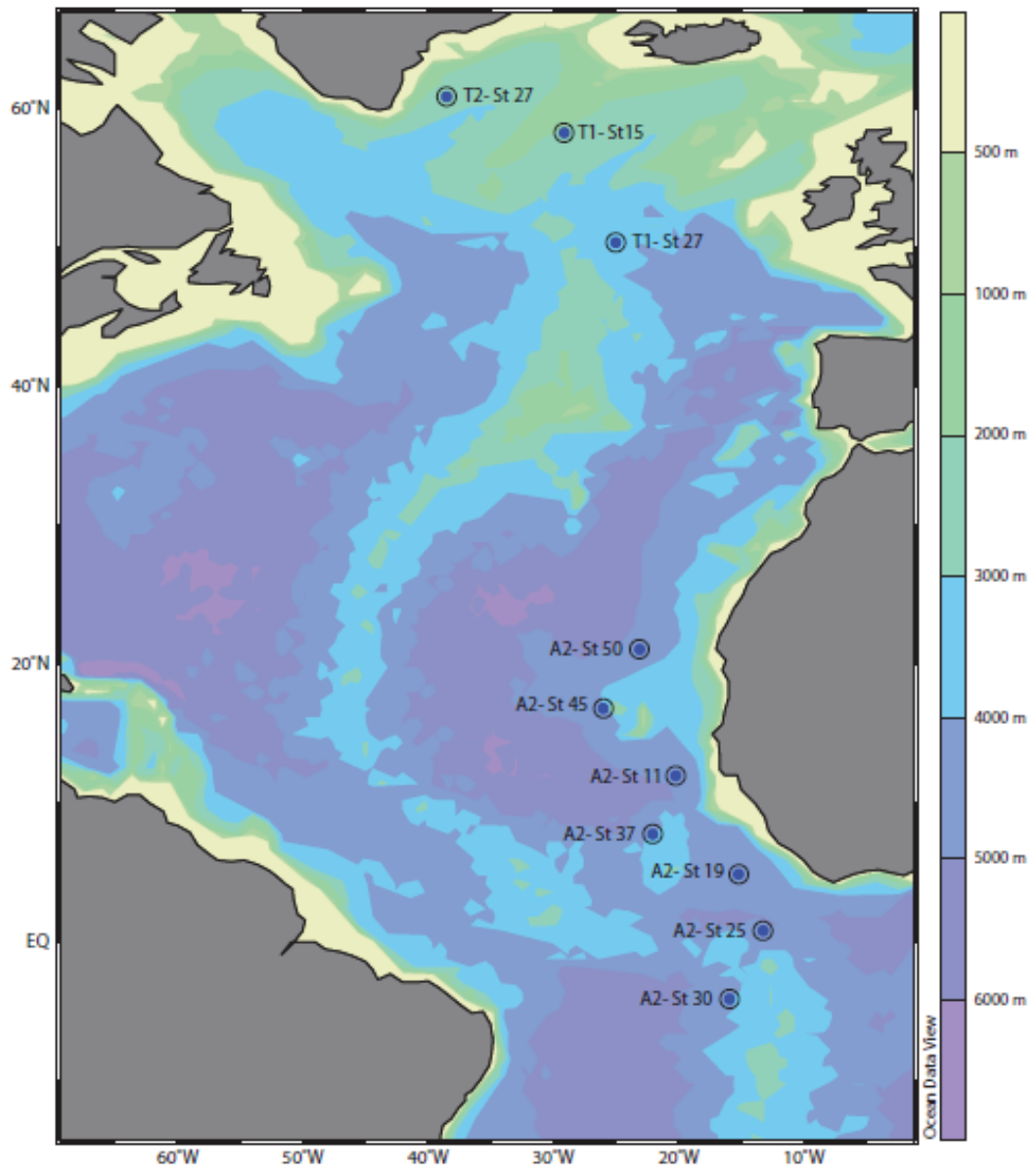


Figure 1.

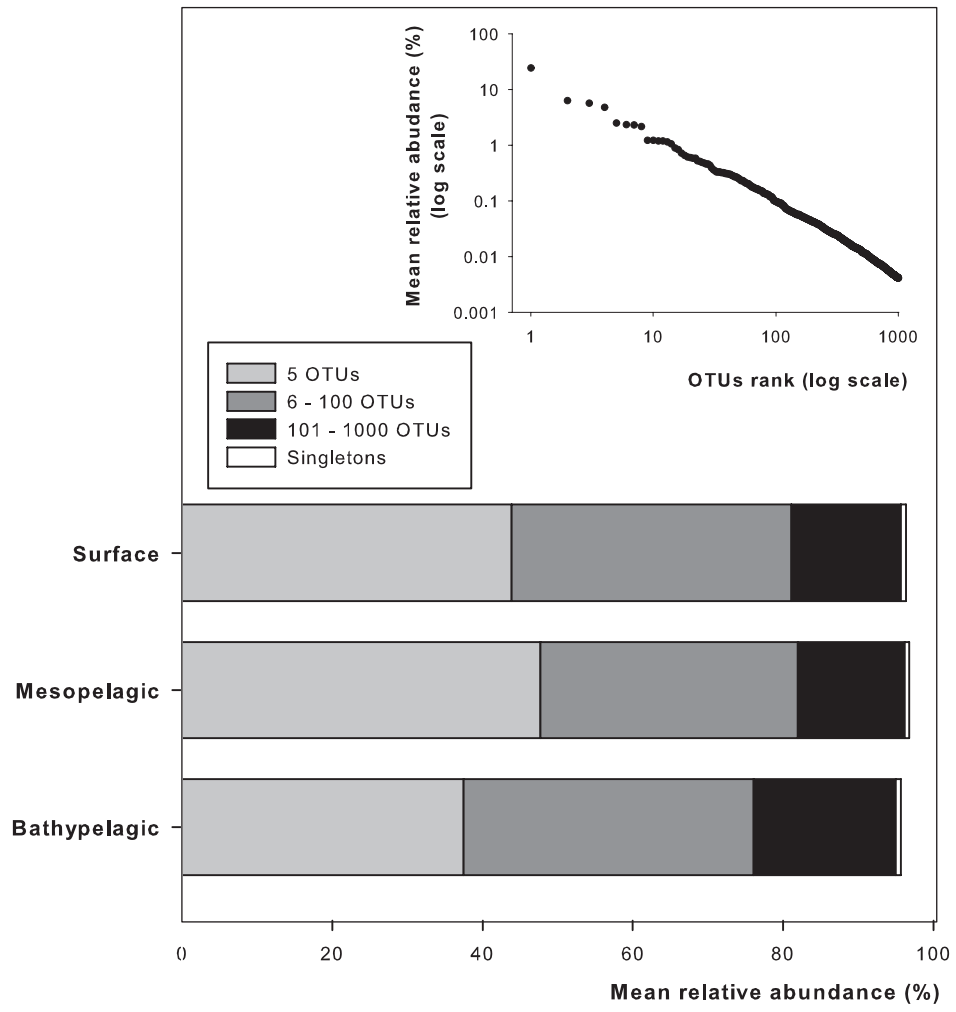


Figure 2.

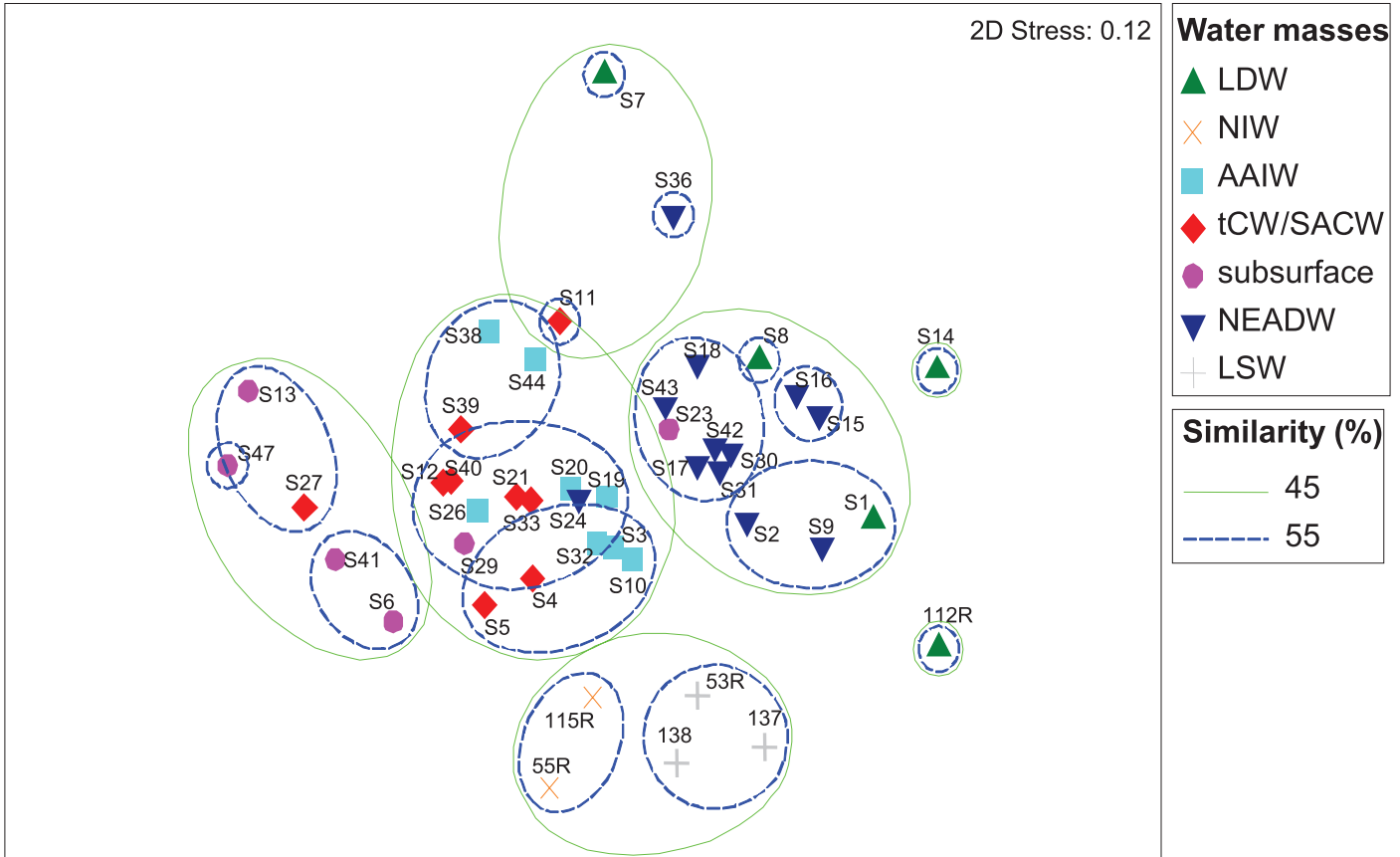


Figure 3.

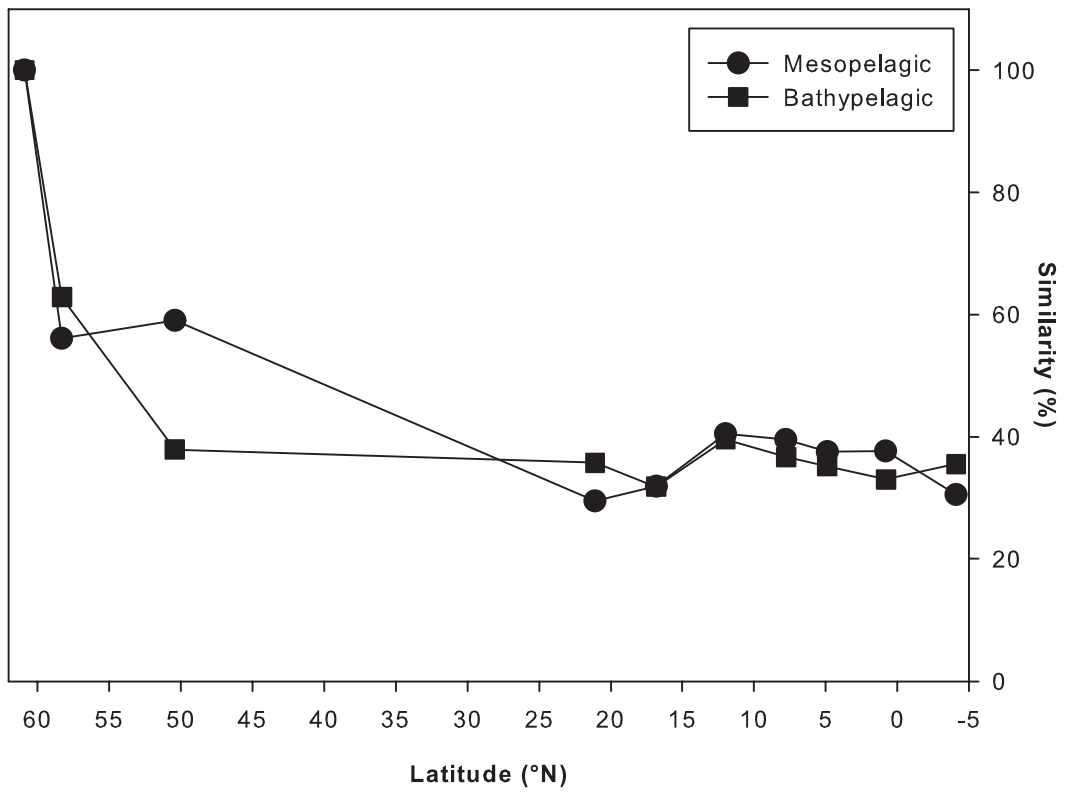


Figure 4.

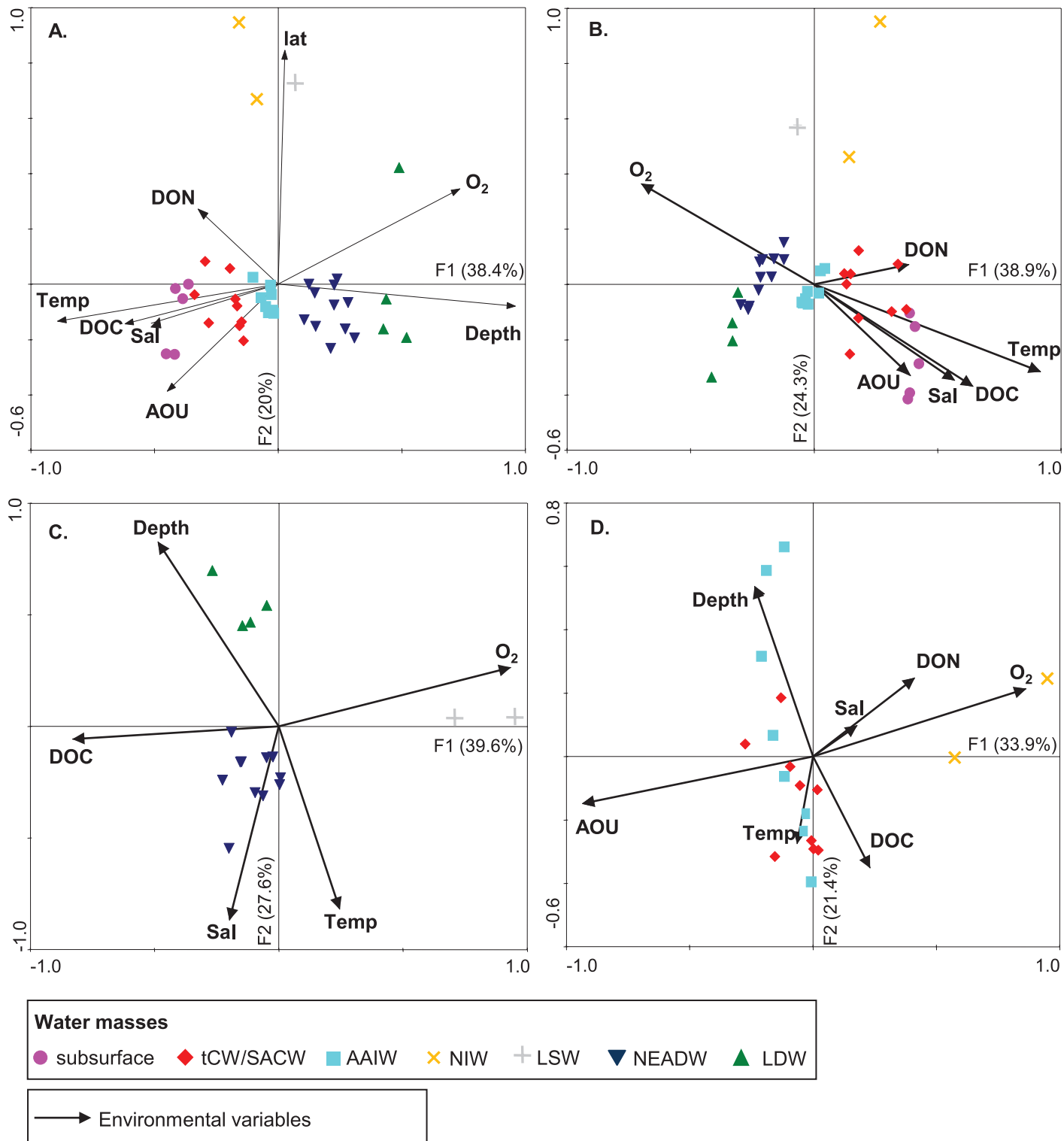


Figure 5.

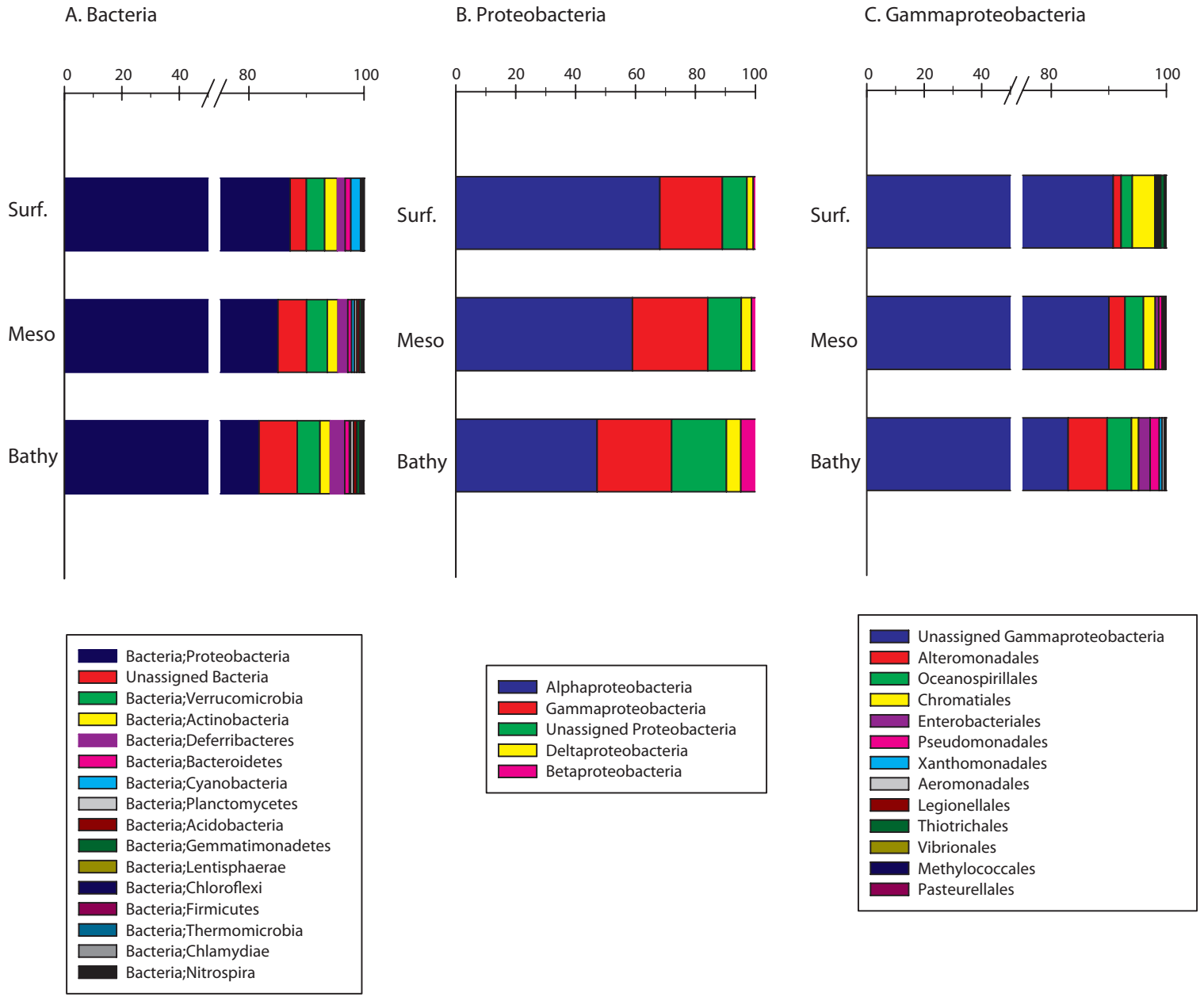


Figure 6.

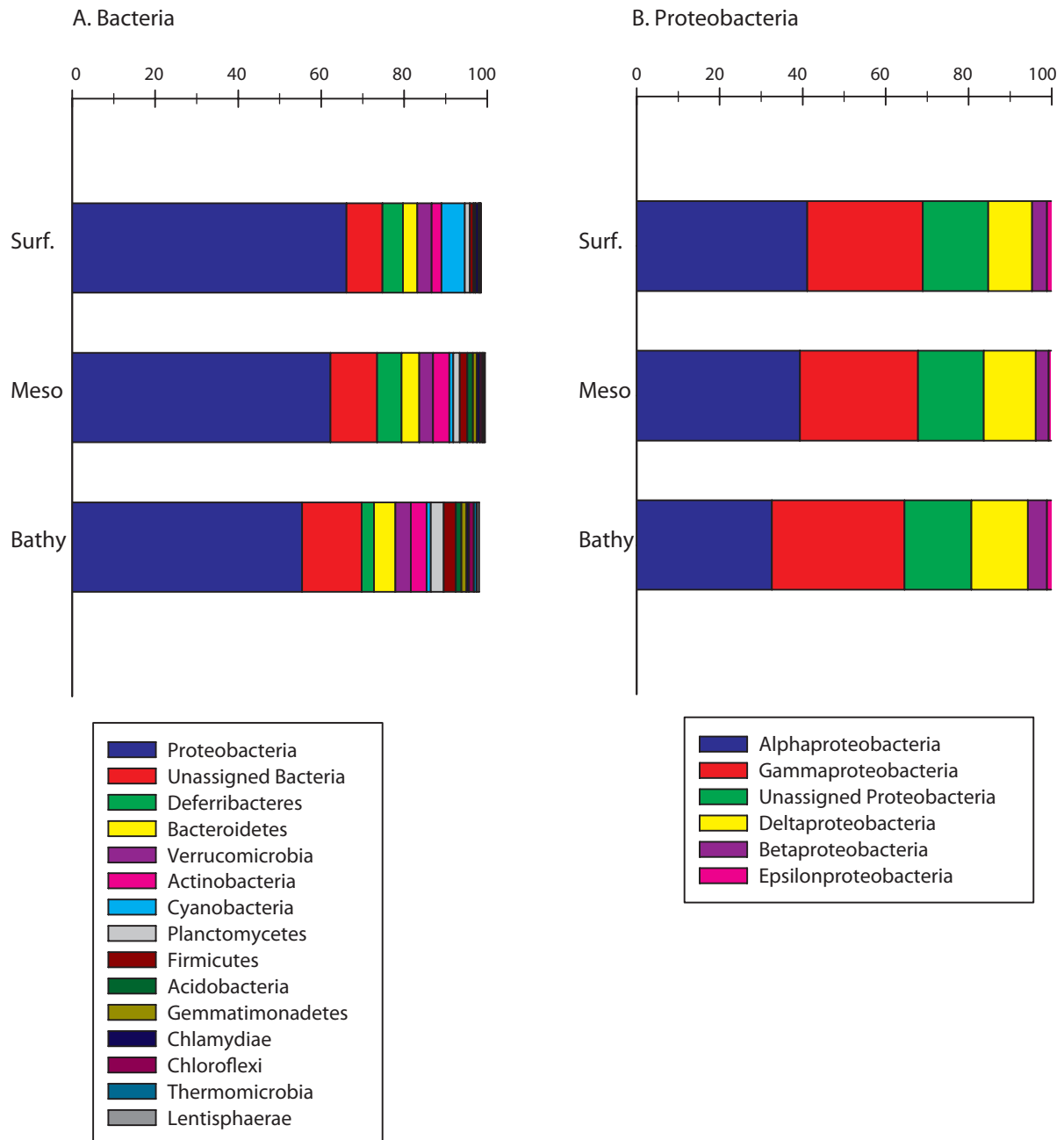


Figure 7.

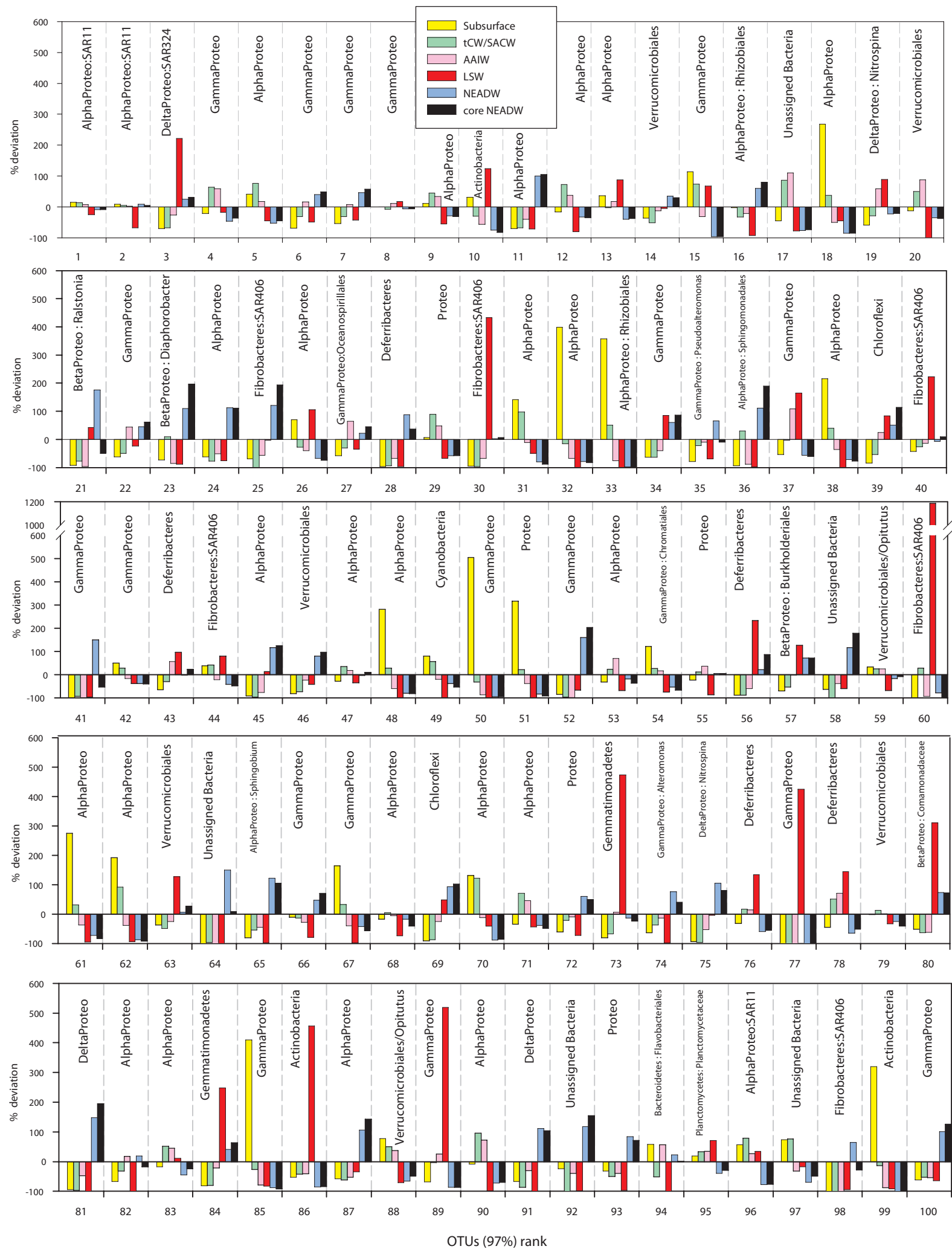


Figure 8.

Supplementary methods.

Environmental parameters

Inorganic nutrients — The methods for determining inorganic nutrient concentrations followed Joint Global Ocean Fluxes Study recommendations (Gordon *et al.* 1993). The concentrations of dissolved inorganic nutrients (NH_4^+ , NO_3^- , NO_2^- , PO_4^{3-}) were determined in a TRAACS autoanalyzer immediately after collecting the samples and gentle filtration through 0.2 μm filters (Acrodisc, Gelman Science). NH_4^+ was detected with the indophenol blue method (pH 10.5) at 630 nm. NO_2^- was detected after diazotation with sulfanilamide and *N*-(1-naphtyl)-ethylene diammonium dichloride as the reddishpurple dye complex at 540 nm. NO_3^- was reduced in a copper cadmium coil to nitrite (with imidazole as a buffer) and then measured as nitrite. Inorganic PO_4^{3-} was determined via the molybdenum blue complex at 880 nm.

Dissolved organic carbon (DOC) — Samples for DOC were filtered through rinsed 0.2 μm polycarbonate filters and sealed in precombusted (450°C for 4 h) glass ampoules after adding 50 μL of 40% phosphoric acid. The samples were stored frozen at -20°C until analysis back in the lab. DOC concentrations of duplicate samples were determined using a Shimadzu TOC-5000 analyzer. Three-point standard curves, prepared with potassium hydrogen phthalate (Nacalai Tesque, Kyoto, Japan), were used to calculate DOC concentrations. The instrument's performance and the validity of the calibration were determined using reference material of the Hansell CRM program (44–46 $\mu\text{mol L}^{-1}$ for the reference samples; $n = 3$ and 1–2 $\mu\text{mol L}^{-1}$ for low carbon water; $n = 3$). The average analytical precision of the instrument was < 3%.

Dissolved organic nitrogen (DON) — Total dissolved nitrogen (TDN) was analyzed with a TRAACS 800 continuous-flow analysis system following the persulfate oxidation method. DON concentrations were calculated by subtracting the sum of the inorganic nitrogen species from

TDN concentrations. The recovery of DON was estimated on a mixture of 10 different organic compounds containing known concentrations of N (Kramer *et al.* 2005). For this reference material, the recovery efficiency of organic nitrogen was 92% of the calculated organic nitrogen concentration.

Bacterial-related parameters

Prokaryotic abundance determined by flow cytometry — Prokaryotic plankton collected from the different depth layers of the water column were enumerated using flow cytometry. Samples (2 ml) were fixed with 1% paraformaldehyde (final concentration), shock-frozen in liquid nitrogen for 5 min and stored at -80°C (Kamiya *et al.* 2007). Picoplankton cells were stained with SYBR-Green I and enumerated with a FACSCalibur flow cytometer (Becton Dickinson) within 2 months. Immediately before analysis, the thawed picoplankton samples were stained with SYBRGreen I at room temperature in the dark for 15 min. Fluorescent microspheres (Molecular Probes) with a diameter of 1 µm were added to all samples as an internal standard. Counts were performed with an argon laser at 488 nm wavelength. Prokaryotic cells were enumerated according to their right angle scatter and green fluorescence. The counting window of the flow cytometer was set to exclude eukaryotic picoplankton.

Prokaryotic heterotrophic production by [³H] leucine incorporation — Bulk PHP was measured by incubating triplicate 10–40 ml samples and formaldehyde-killed blanks (2% final concentration) with 10 nM [³H]-leucine (final concentration, specific activity 160 Ci mmol⁻¹; Amersham) in temperature-controlled incubators in the dark at *in situ* temperature for 4–10 h (Kirchman *et al.* 1985). Incubations were terminated by adding formaldehyde (2% final concentration) before filtering the samples and the blanks through 0.2 µm polycarbonate filters (25 mm filter diameter; Millipore). Subsequently, the filters were rinsed three times with 5% ice-

cold trichloroacetic acid, dried and placed in scintillation vials. Scintillation cocktail (8 ml Canberra-Packard Filter Count) was added, and after 18 h, counted in a liquid scintillation counter (LKB Wallac model 1212). The mean disintegrations per minute (DPM) of the formaldehyde-fixed blanks were subtracted from the mean DPM of the respective samples, and the resulting DPM converted into leucine incorporation rates. Prokaryotic carbon biomass production was estimated using a conservative theoretical conversion factor of $1.55 \text{ kg C mol}^{-1} \text{ Leu}$ assuming no internal isotope dilution (Kirchman & Ducklow 1993).

Activity of the ETS — Electron transport system (ETS) activity was measured following the modifications of the tetrazolium reduction technique as described earlier (Aristegui & Montero 1995). Some minor modifications of the method were made to increase its sensitivity (Baltar *et al.* 2009).

Measurements of prokaryotic extracellular enzymatic activity — The hydrolysis of the fluorogenic substrate analogues 4-methylcoumarinyl-7-amide (MCA)-L-leucine-7-amido-4-methylcoumarin, 4-methylumbelliferyl (MUF)- α -D-glucoside, 4-MUF- β -D-glucoside and MUF-phosphate was measured to estimate potential activity rates of α -, β -glucosidase, aminopeptidase and alkaline phosphatase, respectively (Baltar *et al.* 2009; Hoppe 1983).

The environmental data used in statistical analysis can be found at: <http://icomm.mbl.edu/microbis>.

References

Aristegui J, Montero MF (1995) The relationship between community respiration and ETS activity in the ocean. *Journal of Plankton Research* **17**, 1563-1571.

- Baltar F, Aristegui J, Gasol JM, Sintes E, Herndl GJ (2009) Evidence of prokaryotic metabolism on suspended particulate organic matter in the dark waters of the subtropical North Atlantic. *Limnology and Oceanography* **54**, 182-193.
- Gordon LI, Jennings J, Ross AA, Krest JM (1993) A suggested protocol for continuous flow automated analysis of seawater nutrients (phosphate, nitrate, nitrite and silicic acid) in the WOCE Hydrographic Program and the Joint Global Ocean Fluxes Study. In: *WOCE Operation manual, WHP Operations and Methods*, p. 52. WOCE Hydrographic Program Office.
- Hoppe H-G (1983) Significance of exoenzymatic activities in the ecology of brackish water: measurements by means of methylumbelliferyl-substrates. *Marine Ecology Progress Series* **11**, 299-308.
- Kamiya E, Izumiyama S, Nishimura M, Mitchell J, Kogure K (2007) Effects of fixation and storage on flow cytometric analysis of marine bacteria. *Journal of Oceanography* **63**, 101-112.
- Kirchman DL, Ducklow HW (1993) Estimating converting factors for thymidine and leucine methods for measuring bacterial production. In: *Handbook of methods in aquatic microbial ecology* (eds. Kemp PF, Sherr BF, Sherr EB, Cole JJ), pp. 513-517. Lewis, Boca Raton.
- Kirchman DL, K'Ness E, Hodson R (1985) Leucine incorporation and its potential as a measure of protein synthesis by bacteria in natural aquatic systems. *Applied and Environmental Microbiology* **49**, 599-607.

Kramer GD, Pausz C, Herndl GJ (2005) Elemental composition of dissolved organic matter and bacterioplankton production in the Faroe-Shetland Channel (North Atlantic). *Deep-Sea Research Part I Oceanographic Research Papers* **52**, 85-97.

Table S1. Description of the 45 samples from the North Atlantic Ocean selected for bacterial pyrosequencing. LDW: Lower Deep Water, NEADW: North East Atlantic Deep Water, AAIW: Antarctic Intermediate Water, tCW/SACW: transitional/South Atlantic Central Water, NIW: Northern Intermediate Water, LSW: Labrador Sea Water).

| Sample ID | Cruise | Station | Longitude °E | Latitude °N | Depth (m) | Water mass |
|-----------|--------------|---------|--------------|-------------|-----------|------------|
| 53R | Transat-1 | 15 | -29.13 | 58.3 | 1400 | LSW |
| 55R | Transat-1 | 15 | -29.13 | 58.3 | 500 | NIW |
| 112R | Transat-1 | 27 | -25 | 50.4 | 4000 | LDW |
| 115R | Transat-1 | 27 | -25 | 50.4 | 500 | NIW |
| 137 | Transat-2 | 27 | -38.52 | 60.9 | 1700 | LSW |
| 138 | Transat-2 | 27 | -38.52 | 60.9 | 700 | LSW |
| S1 | Archimedes-2 | 11 | -20.21 | 11.98 | 4000 | LDW |
| S2 | Archimedes-2 | 11 | -20.21 | 11.98 | 2750 | NEADW |
| S3 | Archimedes-2 | 11 | -20.21 | 11.98 | 900 | AAIW |
| S4 | Archimedes-2 | 11 | -20.21 | 11.98 | 500 | tCW |
| S5 | Archimedes-2 | 11 | -20.21 | 11.98 | 250 | tCW |
| S6 | Archimedes-2 | 11 | -20.21 | 11.98 | 100 | Subsurface |
| S7 | Archimedes-2 | 19 | -15.19 | 4.9 | 4500 | LDW |
| S8 | Archimedes-2 | 19 | -15.19 | 4.9 | 4000 | LDW |
| S9 | Archimedes-2 | 19 | -15.19 | 4.9 | 2750 | NEADW |
| S10 | Archimedes-2 | 19 | -15.19 | 4.9 | 900 | AAIW |
| S11 | Archimedes-2 | 19 | -15.19 | 4.9 | 500 | SACW |
| S12 | Archimedes-2 | 19 | -15.19 | 4.9 | 250 | SACW |
| S13 | Archimedes-2 | 19 | -15.19 | 4.9 | 100 | Subsurface |
| S14 | Archimedes-2 | 25 | -13.24 | 0.81 | 4500 | LDW |
| S15 | Archimedes-2 | 25 | -13.24 | 0.81 | 3500 | NEADW |
| S16 | Archimedes-2 | 25 | -13.24 | 0.81 | 3000 | NEADW |
| S17 | Archimedes-2 | 25 | -13.24 | 0.81 | 2000 | NEADW |
| S18 | Archimedes-2 | 25 | -13.24 | 0.81 | 1800 | NEADW |
| S19 | Archimedes-2 | 25 | -13.24 | 0.81 | 900 | AAIW |
| S20 | Archimedes-2 | 25 | -13.24 | 0.81 | 750 | AAIW |
| S21 | Archimedes-2 | 25 | -13.24 | 0.81 | 500 | SACW |
| S23 | Archimedes-2 | 25 | -13.24 | 0.81 | 100 | Subsurface |
| S24 | Archimedes-2 | 30 | -13.24 | 0.81 | 2500 | NEADW |
| S26 | Archimedes-2 | 30 | -15.91 | -4.09 | 750 | AAIW |
| S27 | Archimedes-2 | 30 | -15.91 | -4.09 | 500 | tCW |
| S29 | Archimedes-2 | 30 | -15.91 | -4.09 | 100 | Subsurface |
| S30 | Archimedes-2 | 37 | -22.05 | 7.78 | 2500 | NEADW |
| S31 | Archimedes-2 | 37 | -22.05 | 7.78 | 1800 | NEADW |
| S32 | Archimedes-2 | 37 | -22.05 | 7.78 | 750 | AAIW |
| S33 | Archimedes-2 | 37 | -22.05 | 7.78 | 500 | tCW |
| S36 | Archimedes-2 | 45 | -26.0 | 16.83 | 2500 | NEADW |
| S38 | Archimedes-2 | 45 | -26.0 | 16.83 | 900 | AAIW |
| S39 | Archimedes-2 | 45 | -26.0 | 16.83 | 500 | tCW |
| S40 | Archimedes-2 | 45 | -26.0 | 16.83 | 250 | tCW |
| S41 | Archimedes-2 | 45 | -26.0 | 16.83 | 100 | Subsurface |
| S42 | Archimedes-2 | 50 | -23.11 | 21.09 | 2500 | NEADW |
| S43 | Archimedes-2 | 50 | -23.11 | 21.09 | 1800 | NEADW |
| S44 | Archimedes-2 | 50 | -23.11 | 21.09 | 900 | AAIW |
| S47 | Archimedes-2 | 50 | -23.11 | 21.09 | 100 | Subsurface |

Table S2. Water mass properties (depth, mean and range of potential temperature and salinity) of the different water type of the North Atlantic (tCW/SACW: transitional/South Atlantic Central Water, AAIW: Antarctic Intermediate Water, NIW: Northern Intermediate Water, LSW: Labrador Sea Water, NEADW: North East Atlantic Deep water, LDW: Lower Deep Water) and number of samples (n).

| Water mass | Depth (m) | Pot .Temp.* (°C) | Range (°C) | Salinity | Range | n |
|-------------------|------------------|-------------------------|-------------------|-----------------|---------------|----------|
| Subsurface | 100 - 150 | 16.7 | 14.2 – 20.6 | 35.97 | 35.45 – 37.06 | 6 |
| tCW/SACW | 250 - 500 | 9.9 | 7.4 – 13.2 | 35.05 | 34.66 – 35.62 | 9 |
| NIW | 500 - 750 | 7.1 | 7.0 – 7.1 | 35.09 | 35.05 – 35.12 | 2 |
| AAIW | 750 - 900 | 5.6 | 4.6 – 6.7 | 34.70 | 34.50 – 34.99 | 8 |
| LSW | 1200 - 2100 | 3.3 | 3.0 – 3.5 | 34.89 | 34.87 – 34.92 | 3 |
| NEADW | 1750 - 4000 | 3.0 | 2.2 – 4.0 | 34.95 | 34.90 – 35.03 | 12 |
| LDW | 4000 - 5000 | 1.9 | 1.5 – 2.3 | 34.88 | 34.84 – 34.92 | 5 |

* Pot. Temp.: potential temperature

Table S3. ANOSIM test between water masses (tCW/SACW: transitional/South Atlantic Central Water, AAIW: Antarctic Intermediate Water, NIW: Northern Intermediate Water, LSW: Labrador Sea Water, NEADW: North East Atlantic Deep water, LDW: Lower Deep Water) based on the relative abundance of all OTUs (97%) except the singletons.

Global R = 0.597; Significance level = 0.001; Number of permutations: 999

| Pairwise tests between water masses | R-value | Significance level | Actual permutations |
|-------------------------------------|---------|--------------------|---------------------|
| Subsurface, AAIW | 0.444 | 0.007 | 999 |
| Subsurface, tCW/SACW | 0.228 | 0.034 | 999 |
| Subsurface, NEADW | 0.722 | 0.002 | 999 |
| Subsurface, LDW | 0.744 | 0.006 | 462 |
| Subsurface, LSW | 0.772 | 0.012 | 84 |
| Subsurface, NIW | 0.51 | 0.036 | 56 |
| AAIW, tCW/SACW | 0.115 | 0.062 (n.s.*) | 999 |
| AAIW, NEADW | 0.428 | 0.001 | 999 |
| AAIW, LDW | 0.796 | 0.002 | 999 |
| AAIW, LSW | 0.874 | 0.006 | 165 |
| AAIW, NIW | 0.716 | 0.022 | 45 |
| tCW/SACW, NEADW | 0.759 | 0.001 | 999 |
| tCW/SACW, LDW | 0.878 | 0.001 | 999 |
| tCW/SACW, LSW | 0.937 | 0.005 | 220 |
| tCW/SACW, NIW | 0.709 | 0.018 | 55 |
| NEADW, LDW | 0.744 | 0.006 | 462 |
| NEADW, LSW | 0.89 | 0.002 | 455 |
| NEADW, NIW | 0.937 | 0.011 | 91 |
| LDW, LSW | 0.508 | 0.036 | 56 |
| LDW, NIW | 0.545 | 0.048 | 21 |
| LSW, NIW | 1 | 0.1 (n.s.*) | 10 |

*n.s.: non-significant

Table S4. Characteristics of the 100 most abundant OTUs (# of OTUs; ID, identification number; percent of contribution to the 100 most abundant OTUs; affiliation)

| # OTU | Cluster ID | % to the 100 first OTUs | Affiliation |
|-------|----------------------------|-------------------------|---|
| 1 | Alphaproteobacteria_03_1 | 29,72 | Bacteria;Proteobacteria;Alphaproteobacteria;Rickettsiales;SAR11 |
| 2 | Alphaproteobacteria_03_2 | 7,87 | Bacteria;Proteobacteria;Alphaproteobacteria;Rickettsiales;SAR11 |
| 3 | ProteobacteriaNA_03_1 | 7,06 | Bacteria;Proteobacteria |
| 4 | Gammaproteobacteria_03_8 | 5,85 | Bacteria;Proteobacteria;Gammaproteobacteria |
| 5 | Alphaproteobacteria_03_21 | 3,08 | Bacteria;Proteobacteria;Alphaproteobacteria |
| 6 | Gammaproteobacteria_03_29 | 2,93 | Bacteria;Proteobacteria;Gammaproteobacteria |
| 7 | Gammaproteobacteria_03_47 | 2,88 | Bacteria;Proteobacteria;Gammaproteobacteria |
| 8 | Gammaproteobacteria_03_44 | 2,69 | Bacteria;Proteobacteria;Gammaproteobacteria |
| 9 | ProteobacteriaNA_03_6 | 1,52 | Bacteria;Proteobacteria |
| 10 | Actinobacteria_03_4 | 1,54 | Bacteria;Actinobacteria;Actinobacteria |
| 11 | ProteobacteriaNA_03_8 | 1,52 | Bacteria;Proteobacteria |
| 12 | Alphaproteobacteria_03_53 | 1,46 | Bacteria;Proteobacteria;Alphaproteobacteria |
| 13 | Alphaproteobacteria_03_26 | 1,41 | Bacteria;Proteobacteria;Alphaproteobacteria |
| 14 | Verrucomicrobia_03_3 | 1,33 | Bacteria;Verrucomicrobia;Verrucomicrobiae;Verrucomicrobiales |
| 15 | Gammaproteobacteria_03_52 | 1,11 | Bacteria;Proteobacteria;Gammaproteobacteria |
| 16 | Alphaproteobacteria_03_258 | 1,03 | Bacteria;Proteobacteria;Alphaproteobacteria;Rhizobiales |
| 17 | BacteriaNA_03_2 | 0,89 | Bacteria |
| 18 | Alphaproteobacteria_03_20 | 0,81 | Bacteria;Proteobacteria;Alphaproteobacteria |
| 19 | Deltaproteobacteria_03_2 | 0,75 | Bacteria;Proteobacteria;Deltaproteobacteria;Desulfobacterales;Nitrospinaceae;Nitrospina |
| 20 | Verrucomicrobia_03_6 | 0,73 | Bacteria;Verrucomicrobia;Verrucomicrobiae;Verrucomicrobiales |
| 21 | Betaproteobacteria_03_1 | 0,87 | Bacteria;Proteobacteria;Betaproteobacteria;Burkholderiales;Burkholderiaceae;Ralstonia |
| 22 | Gammaproteobacteria_03_106 | 0,72 | Bacteria;Proteobacteria;Gammaproteobacteria |
| 23 | Betaproteobacteria_03_11 | 0,74 | Bacteria;Proteobacteria;Betaproteobacteria;Burkholderiales;Comamonadaceae;Diaphorobacter |
| 24 | ProteobacteriaNA_03_14 | 0,64 | Bacteria;Proteobacteria |
| 25 | BacteriaNA_03_15 | 0,62 | Bacteria |
| 26 | Alphaproteobacteria_03_17 | 0,60 | Bacteria;Proteobacteria;Alphaproteobacteria |
| 27 | Gammaproteobacteria_03_78 | 0,57 | Bacteria;Proteobacteria;Gammaproteobacteria;Oceanospirillales |
| 28 | Deferribacteres_03_6 | 0,61 | Bacteria;Deferribacteres |
| 29 | ProteobacteriaNA_03_12 | 0,53 | Bacteria;Proteobacteria |
| 30 | BacteriaNA_03_6 | 0,49 | Bacteria |
| 31 | Alphaproteobacteria_03_94 | 0,45 | Bacteria;Proteobacteria;Alphaproteobacteria |
| 32 | Alphaproteobacteria_03_71 | 0,44 | Bacteria;Proteobacteria;Alphaproteobacteria |
| 33 | Alphaproteobacteria_03_261 | 0,40 | Bacteria;Proteobacteria;Alphaproteobacteria;Rhizobiales |
| 34 | Gammaproteobacteria_03_128 | 0,41 | Bacteria;Proteobacteria;Gammaproteobacteria |
| 35 | Gammaproteobacteria_03_7 | 0,41 | Bacteria;Proteobacteria;Gammaproteobacteria;Alteromonadales;Pseudoalteromonadaceae;Pseudoalteromona |
| 36 | Alphaproteobacteria_03_27 | 0,45 | Bacteria;Proteobacteria;Alphaproteobacteria;Sphingomonadales;Sphingomonadaceae |
| 37 | Gammaproteobacteria_03_113 | 0,39 | Bacteria;Proteobacteria;Gammaproteobacteria |
| 38 | Alphaproteobacteria_03_30 | 0,39 | Bacteria;Proteobacteria;Alphaproteobacteria |
| 39 | BacteriaNA_03_10 | 0,39 | Bacteria |
| 40 | BacteriaNA_03_14 | 0,38 | Bacteria |
| 41 | Gammaproteobacteria_03_19 | 0,43 | Bacteria;Proteobacteria;Gammaproteobacteria |
| 42 | Gammaproteobacteria_03_40 | 0,38 | Bacteria;Proteobacteria;Gammaproteobacteria |
| 43 | Deferribacteres_03_10 | 0,37 | Bacteria;Deferribacteres |
| 44 | BacteriaNA_03_49 | 0,36 | Bacteria |
| 45 | Alphaproteobacteria_03_116 | 0,36 | Bacteria;Proteobacteria;Alphaproteobacteria |
| 46 | Verrucomicrobia_03_17 | 0,35 | Bacteria;Verrucomicrobia;Verrucomicrobiae;Verrucomicrobiales;Verrucomicrobiaceae |
| 47 | Alphaproteobacteria_03_159 | 0,34 | Bacteria;Proteobacteria;Alphaproteobacteria |
| 48 | Alphaproteobacteria_03_75 | 0,33 | Bacteria;Proteobacteria;Alphaproteobacteria |
| 49 | Cyanobacteria_03_1 | 0,32 | Bacteria;Cyanobacteria;True Cyanobacteria;Prochlorales |

| | | | |
|-----|----------------------------|------|--|
| 50 | Gammaproteobacteria_03_130 | 0,31 | Bacteria;Proteobacteria;Gammaproteobacteria |
| 51 | ProteobacteriaNA_03_7 | 0,30 | Bacteria;Proteobacteria |
| 52 | Gammaproteobacteria_03_270 | 0,30 | Bacteria;Proteobacteria;Gammaproteobacteria |
| 53 | Alphaproteobacteria_03_169 | 0,29 | Bacteria;Proteobacteria;Alphaproteobacteria |
| 54 | Gammaproteobacteria_03_9 | 0,28 | Bacteria;Proteobacteria;Gammaproteobacteria;Chromatiales;Ectothiorhodospiraceae |
| 55 | ProteobacteriaNA_03_22 | 0,28 | Bacteria;Proteobacteria |
| 56 | Deferribacteres_03_11 | 0,27 | Bacteria;Deferribacteres |
| 57 | Betaproteobacteria_03_3 | 0,28 | Bacteria;Proteobacteria;Betaproteobacteria;Burkholderiales;Comamonadaceae |
| 58 | BacteriaNA_03_18 | 0,26 | Bacteria |
| 59 | Verrucomicrobia_03_45 | 0,25 | Bacteria;Verrucomicrobia;Opitutae;Opitales;Opitutaceae;Opitutus |
| 60 | BacteriaNA_03_4 | 0,24 | Bacteria |
| 61 | Alphaproteobacteria_03_79 | 0,24 | Bacteria;Proteobacteria;Alphaproteobacteria |
| 62 | Alphaproteobacteria_03_52 | 0,23 | Bacteria;Proteobacteria;Alphaproteobacteria |
| 63 | Verrucomicrobia_03_29 | 0,23 | Bacteria;Verrucomicrobia;Verrucomicrobiae;Verrucomicrobiales |
| 64 | BacteriaNA_03_41 | 0,23 | Bacteria |
| 65 | Alphaproteobacteria_03_18 | 0,24 | Bacteria;Proteobacteria;Alphaproteobacteria;Sphingomonadales;Sphingomonadaceae;Sphingobium |
| 66 | Gammaproteobacteria_03_206 | 0,21 | Bacteria;Proteobacteria;Gammaproteobacteria |
| 67 | Gammaproteobacteria_03_25 | 0,21 | Bacteria;Proteobacteria;Gammaproteobacteria |
| 68 | Alphaproteobacteria_03_14 | 0,21 | Bacteria;Proteobacteria;Alphaproteobacteria |
| 69 | BacteriaNA_03_35 | 0,21 | Bacteria |
| 70 | Alphaproteobacteria_03_242 | 0,20 | Bacteria;Proteobacteria;Alphaproteobacteria |
| 71 | Alphaproteobacteria_03_155 | 0,20 | Bacteria;Proteobacteria;Alphaproteobacteria |
| 72 | ProteobacteriaNA_03_25 | 0,20 | Bacteria;Proteobacteria |
| 73 | Gemmatimonadetes_03_3 | 0,18 | Bacteria;Gemmatimonadetes |
| 74 | Gammaproteobacteria_03_15 | 0,19 | Bacteria;Proteobacteria;Gammaproteobacteria;Alteromonadales;Alteromonadaceae;Alteromonas |
| 75 | Deltaproteobacteria_03_106 | 0,19 | Bacteria;Proteobacteria;Deltaproteobacteria;Desulfobacterales;Nitrospinaceae;Nitrospina |
| 76 | Deferribacteres_03_7 | 0,19 | Bacteria;Deferribacteres |
| 77 | Gammaproteobacteria_03_83 | 0,18 | Bacteria;Proteobacteria;Gammaproteobacteria |
| 78 | Deferribacteres_03_4 | 0,18 | Bacteria;Deferribacteres |
| 79 | Verrucomicrobia_03_28 | 0,17 | Bacteria;Verrucomicrobia;Verrucomicrobiae;Verrucomicrobiales |
| 80 | Betaproteobacteria_03_9 | 0,18 | Bacteria;Proteobacteria;Betaproteobacteria;Burkholderiales;Comamonadaceae |
| 81 | Deltaproteobacteria_03_122 | 0,17 | Bacteria;Proteobacteria;Deltaproteobacteria |
| 82 | Alphaproteobacteria_03_32 | 0,17 | Bacteria;Proteobacteria;Alphaproteobacteria |
| 83 | Alphaproteobacteria_03_329 | 0,17 | Bacteria;Proteobacteria;Alphaproteobacteria |
| 84 | Gemmatimonadetes_03_1 | 0,17 | Bacteria;Gemmatimonadetes |
| 85 | Gammaproteobacteria_03_46 | 0,17 | Bacteria;Proteobacteria;Gammaproteobacteria |
| 86 | Actinobacteria_03_32 | 0,15 | Bacteria;Actinobacteria;Actinobacteria |
| 87 | Alphaproteobacteria_03_264 | 0,16 | Bacteria;Proteobacteria;Alphaproteobacteria |
| 88 | Verrucomicrobia_03_19 | 0,16 | Bacteria;Verrucomicrobia;Opitutae;Opitales;Opitutaceae;Opitutus |
| 89 | Gammaproteobacteria_03_198 | 0,14 | Bacteria;Proteobacteria;Gammaproteobacteria |
| 90 | Alphaproteobacteria_03_195 | 0,15 | Bacteria;Proteobacteria;Alphaproteobacteria |
| 91 | Deltaproteobacteria_03_74 | 0,15 | Bacteria;Proteobacteria;Deltaproteobacteria |
| 92 | BacteriaNA_03_38 | 0,15 | Bacteria |
| 93 | ProteobacteriaNA_03_51 | 0,14 | Bacteria;Proteobacteria |
| 94 | Bacteroidetes_03_18 | 0,15 | Bacteria;Bacteroidetes;Flavobacteria;Flavobacteriales |
| 95 | Planctomycetes_03_6 | 0,13 | Bacteria;Planctomycetes;Planctomycetacia;Planctomycetales;Planctomycetaceae |
| 96 | Alphaproteobacteria_03_280 | 0,12 | Bacteria;Proteobacteria;Alphaproteobacteria;Rickettsiales;SAR11 |
| 97 | BacteriaNA_03_21 | 0,13 | Bacteria |
| 98 | BacteriaNA_03_75 | 0,14 | Bacteria |
| 99 | Actinobacteria_03_37 | 0,13 | Bacteria;Actinobacteria;Actinobacteria |
| 100 | Gammaproteobacteria_03_32 | 0,12 | Bacteria;Proteobacteria;Gammaproteobacteria |

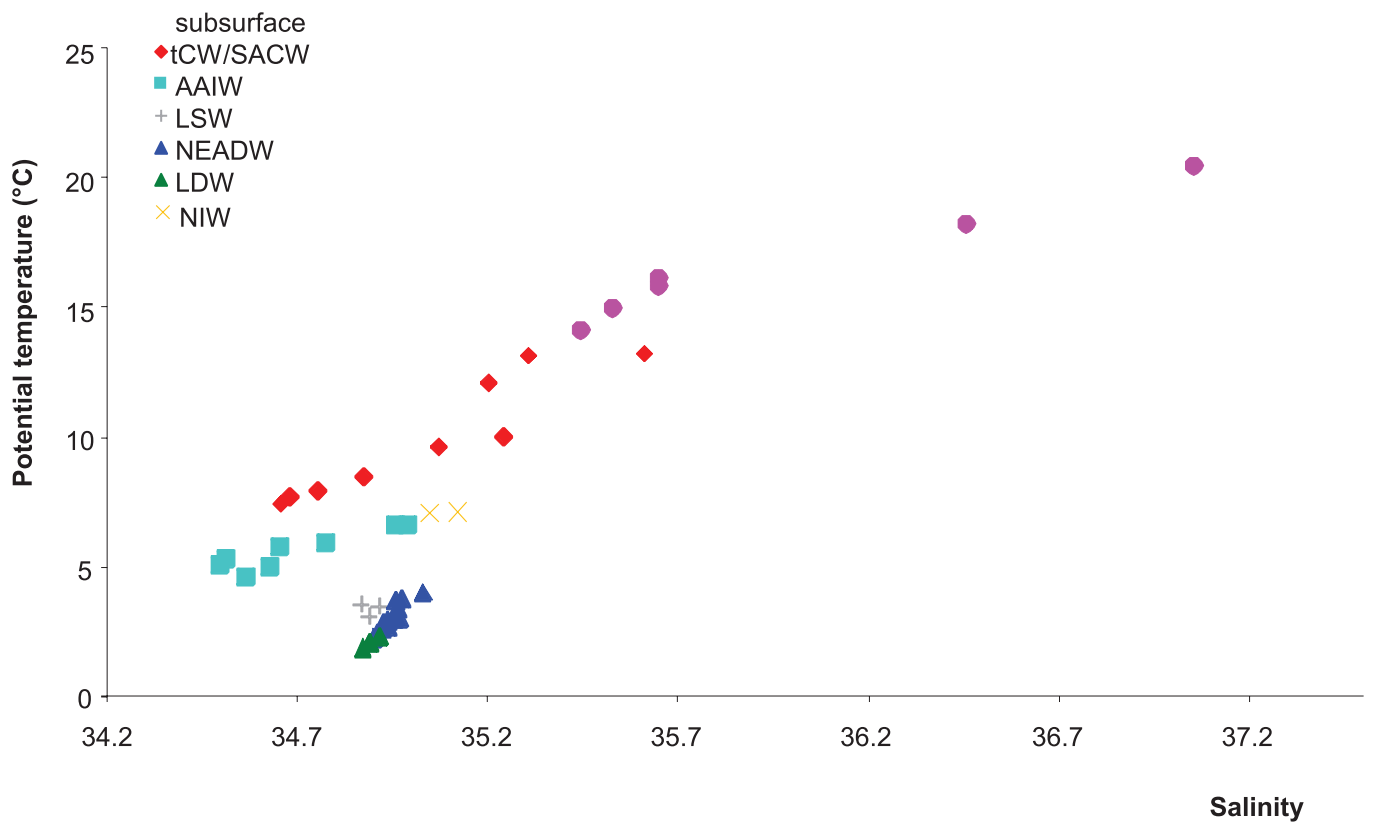


Figure S1. Temperature – salinity diagram based on all the samples. Different symbols indicate the different water masses (tCW/SACW: transitional/South Atlantic Central Water, AAIW: Antarctic Intermediate Water, LSW: Labrador Sea Water, NEADW: North East Atlantic Deep Water, LDW: Lower Deep Water).

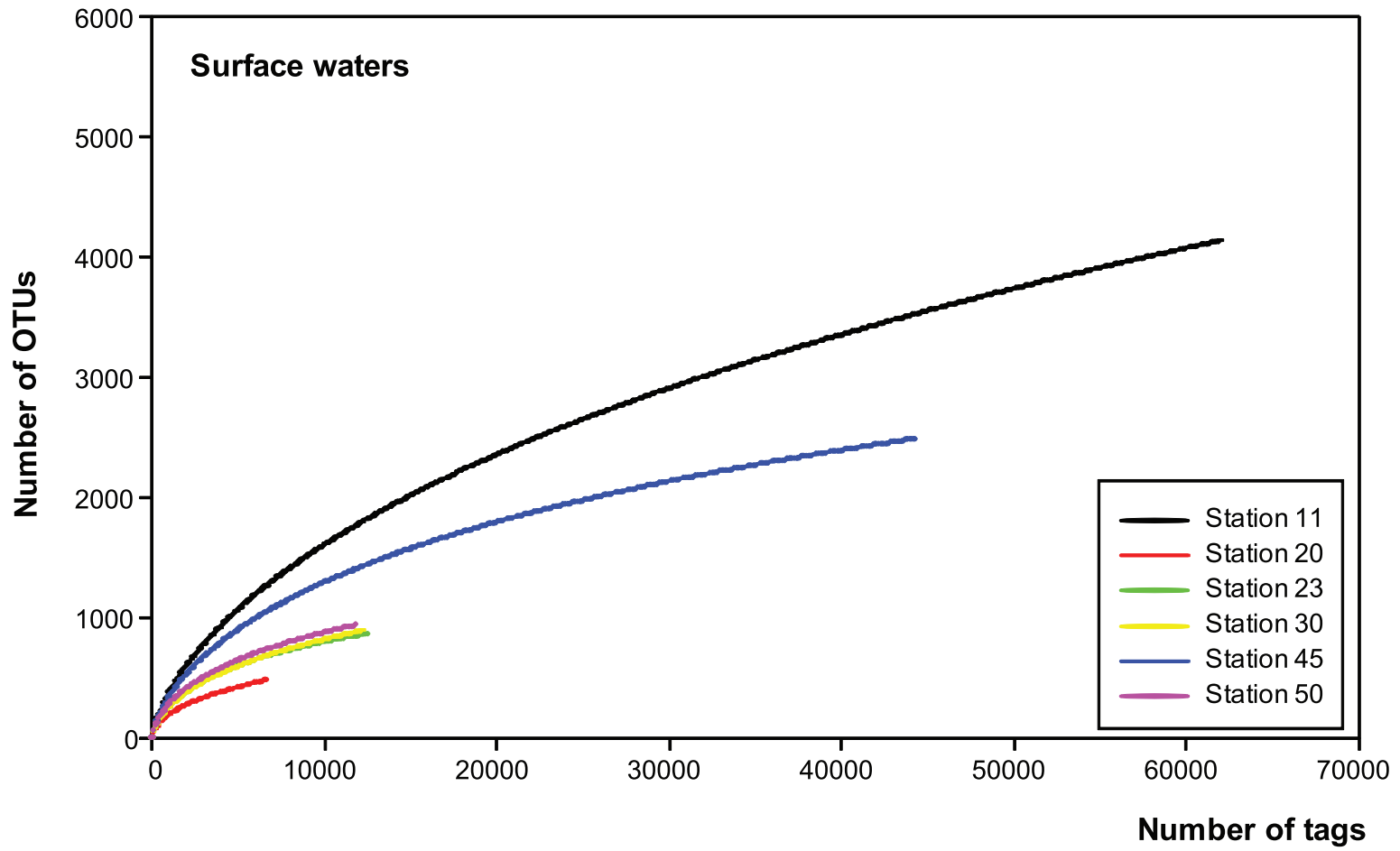


Figure S2 A. Rarefaction curves for subsurface (≈ 100 m depth) samples.

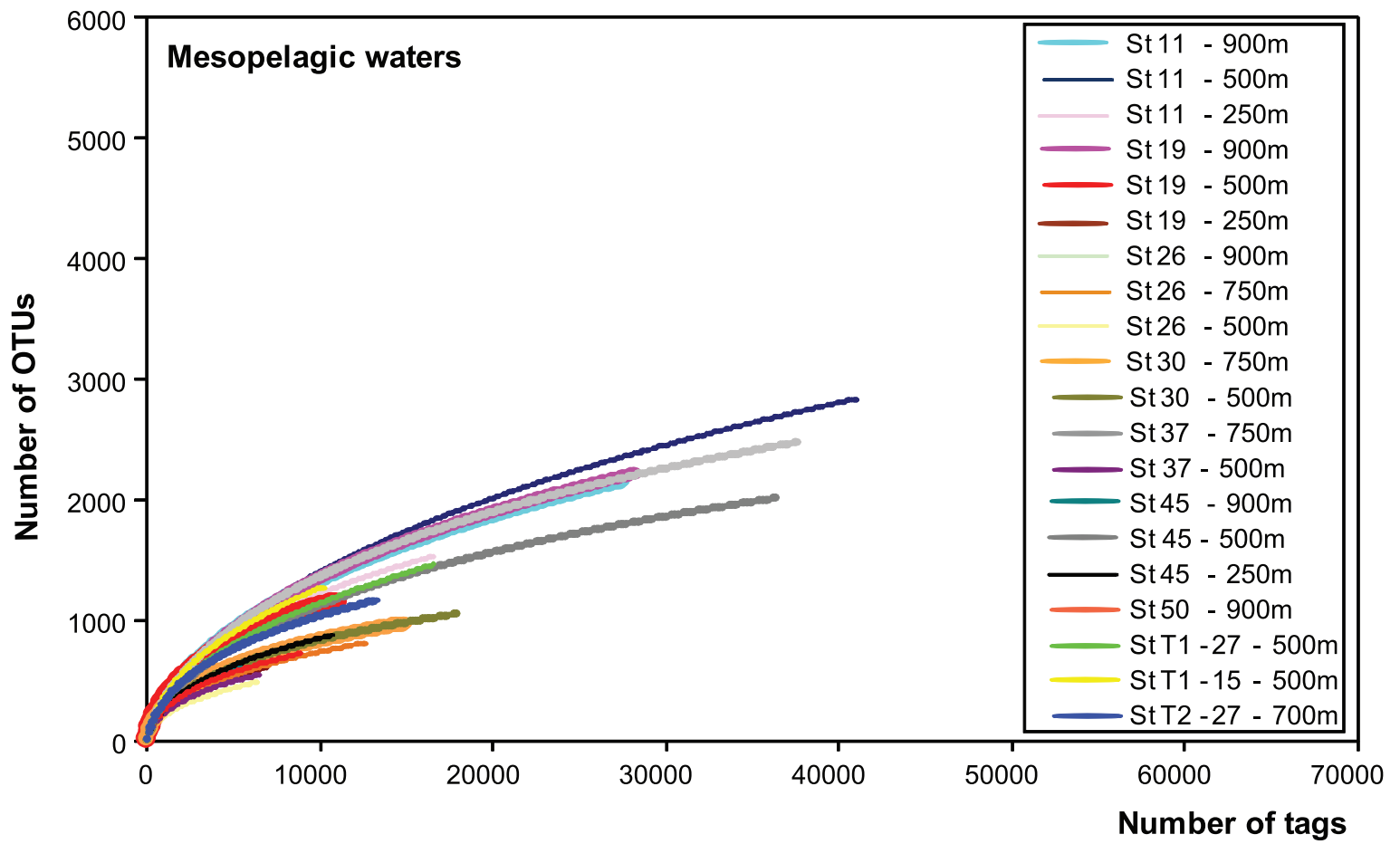


Figure S2 B. Rarefaction curves for mesopelagic samples.

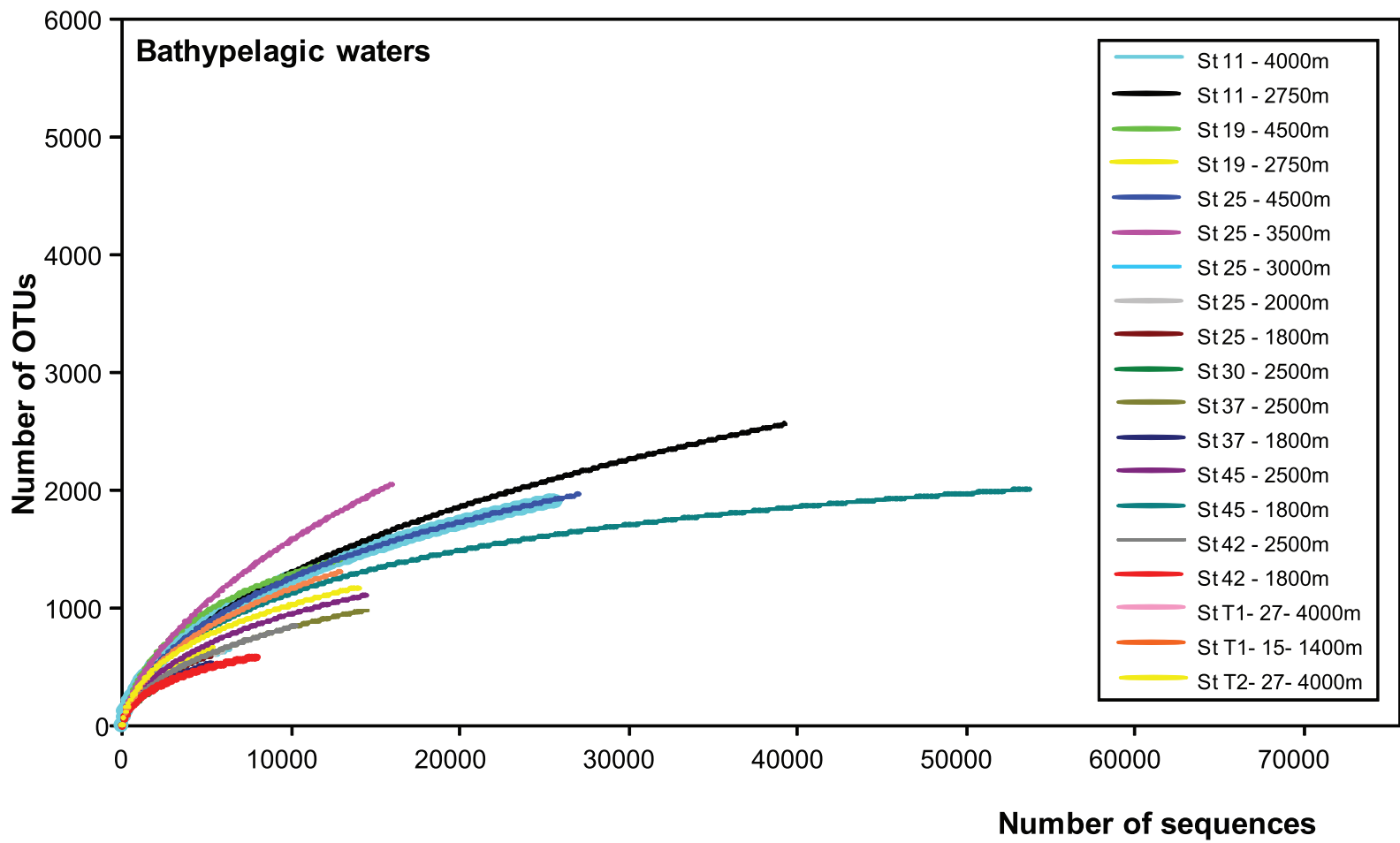


Figure S2 C. Rarefaction curves for bathypelagic samples.

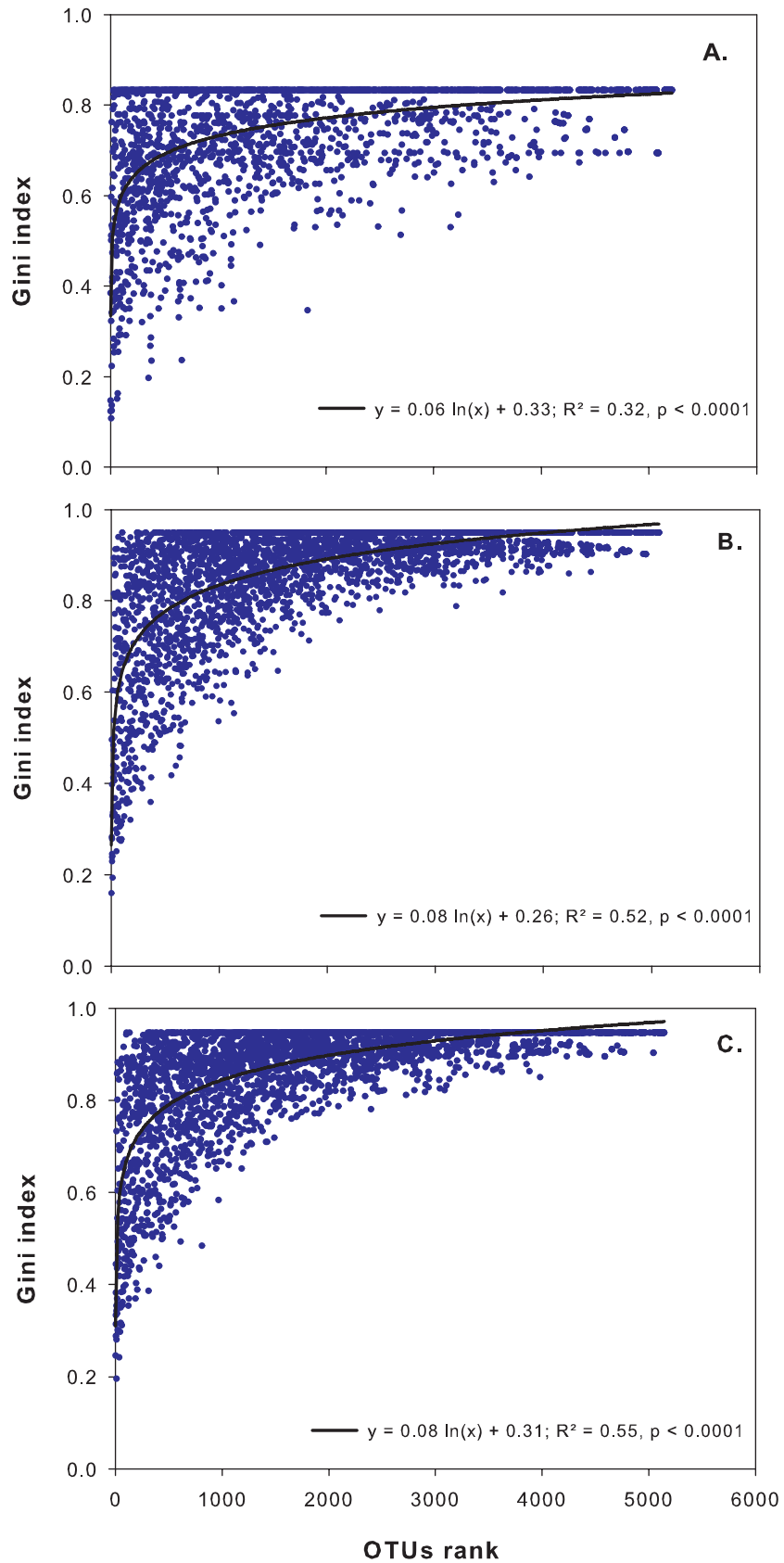


Figure S3. Evenness (Gini index) for each bacterial OTUs (97%) except the singletons from (A) subsurface, (B) mesopelagic and (C) bathypelagic samples vs. the rank (based on the relative abundance) of that OTU. A Gini index of 1 would indicate a very uneven OTU whereas a Gini index of 0 would indicate a perfectly even OTU.

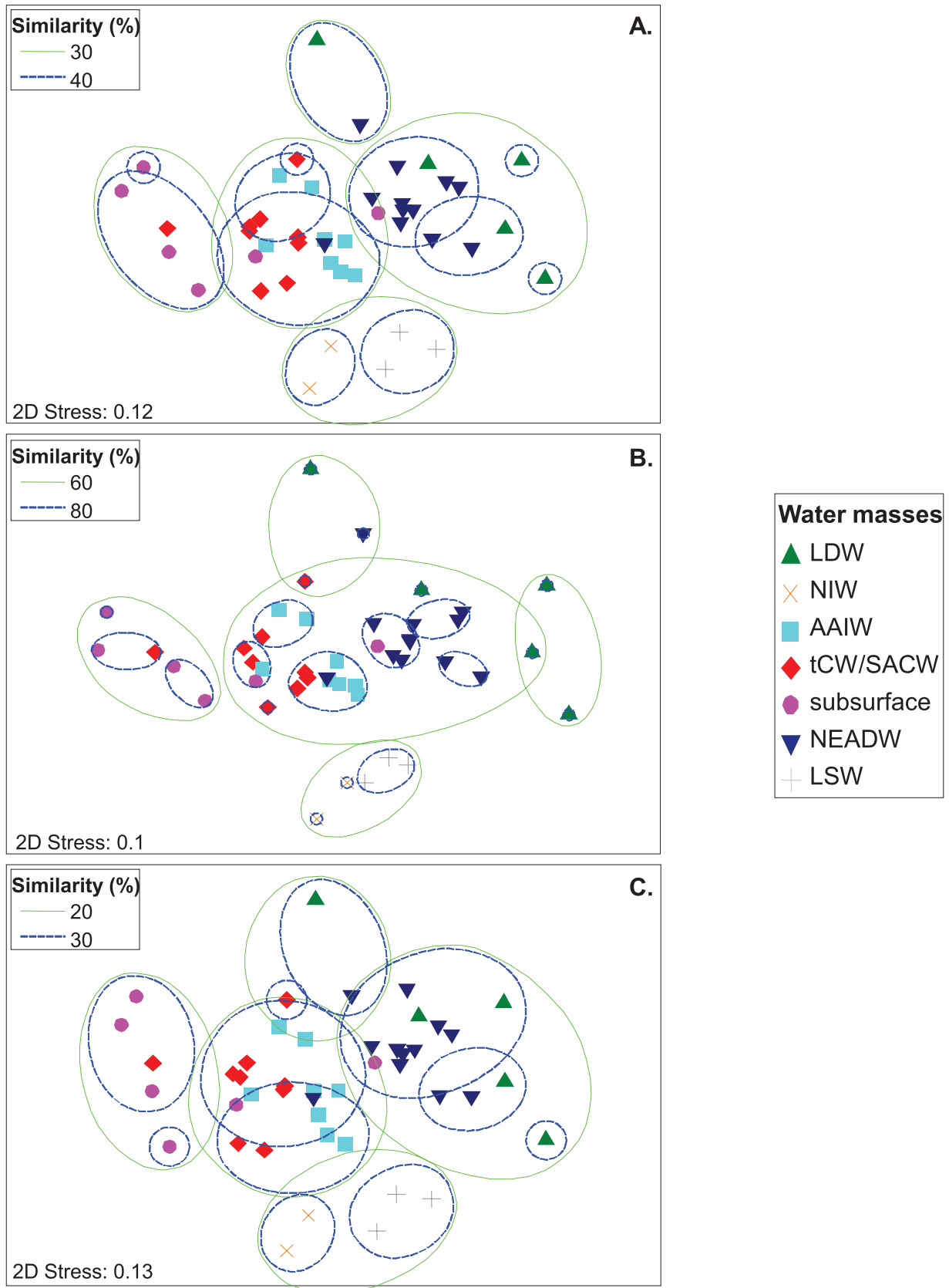


Figure S4. Non-metric multidimensional analysis based on relative abundance of (A) all pyrotags except the singletons, (B) abundant pyrotags (frequency > 1% within a sample) and (C) rare pyrotags (frequency < 0.1% within a sample). Individual samples were affiliated to their respective water-mass. Superimposed circles represent clusters of samples at similarity values of (A) 30 and 40%, (B) 60 and 80% and (C) 20 and 30% (Bray-Curtis similarity). The final solution was based on 25 iterations with a final stress of (a) 0.10 and (b) 0.13.

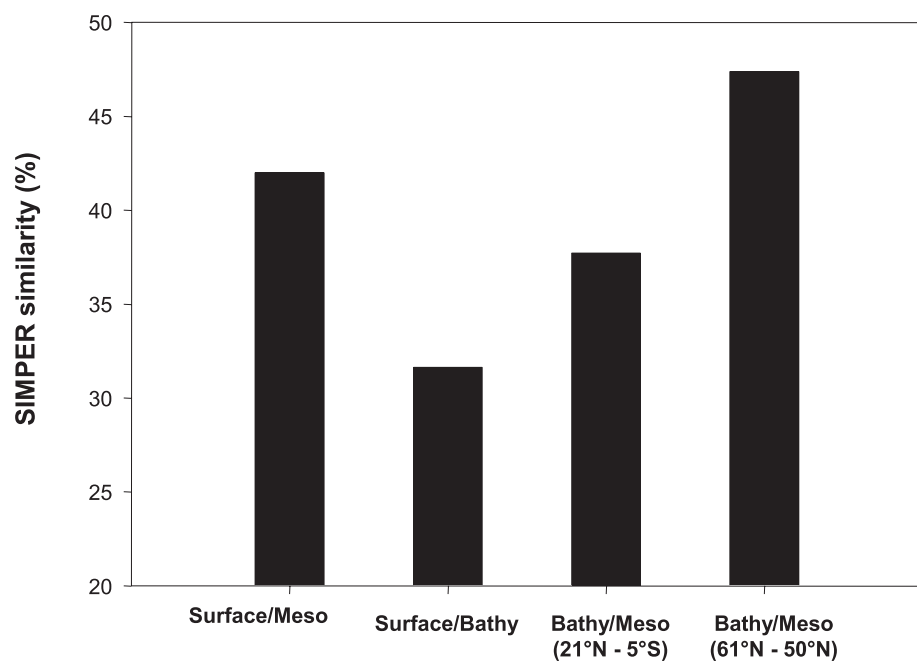


Figure S5. Percent of similarity (calculated through SIMPER analysis) between depth zones.